Pinhead signaling regulates mesoderm heterogeneity via FGF receptor-dependent pathway

Olga Ossipova[#], Keiji Itoh[#], Aurelian Radu, Jerome Ezan[‡] and Sergei Y. Sokol*

Department of Cell, Developmental and Regenerative Biology,

Icahn School of Medicine at Mount Sinai, New York

*Correspondence: Sergei Y. Sokol, Ph. D.,

Phone: 1-212-241-1757; Fax: 1-212-860-9279

E-mail: sergei.sokol@mssm.edu

[#] Equal contribution

[‡]Current address: Université de Bordeaux, Neurocentre Magendie, INSERM U1215, Bordeaux 33077, France.

Abstract

Among the three embryonic germ layers, mesoderm plays a central role in the establishment of the vertebrate body plan. Mesoderm is specified by secreted signaling proteins from the FGF, Nodal, BMP and Wnt families. No new classes of extracellular mesoderm-inducing factors have been identified in more than two decades. Here we show that the pinhead (*pnhd)* gene encodes a secreted protein that is essential for the activation of a subset of mesodermal markers in the *Xenopus* embryo. RNA sequencing revealed that many transcriptional targets of Pnhd are shared with those of the FGF pathway. Pnhd activity was accompanied by Erk phosphorylation and required FGF and Nodal but not Wnt signaling. We propose that during gastrulation Pnhd acts in the marginal zone to contribute to mesoderm heterogeneity via an FGF receptor-dependent positive feedback mechanism.

Keywords

Wnt, FGF, Erk1, Akt, Brachyury, Nodal, antero-posterior axis, Xenopus

Introduction

Vertebrate embryonic body plan forms via the specification of three germ layers, ectoderm, mesoderm and endoderm. Mesoderm plays a central role in this process, being responsible for tissue patterning and cell movements during gastrulation. At late blastula stages, mesoderm (or more precisely, mesendoderm (Rodaway and Patient, 2001) is characterized by the dorsoanterior and ventroposterior domains of gene expression. The dorsoanterior domain marks the signaling center known as Spemann organizer that gives rise to dorsal mesoderm and modulates all three germ layers**.** Factors secreted from the organizer induce neural tissue in the ectoderm and subdivide mesoderm into dorsal (notochord), paraxial (somites), intermediate (kidney and gonads) and lateral/ventral (e. g., blood) types. Signals from the ventrolateral marginal zone and vegetal endoderm also contribute to mesoderm patterning (De Robertis and Kuroda, 2004; Harland and Gerhart, 1997; Kiecker et al., 2016; Langdon and Mullins, 2011; Niehrs, 2004; Zorn and Wells, 2009).

Studies of the past three decades extensively characterized the signaling pathways that contribute to the formation of the three germ layers and specify the primary embryonic axis (Harland and Gerhart, 1997). Only a handful of secreted signaling molecules from the FGF, Wnt, Nodal and BMP families have been shown involved in mesoderm induction and patterning (Christen and Slack, 1999; Kiecker et al., 2016; Kimelman, 2006; Schohl and Fagotto, 2002). *Pinhead* (*pnhd)* has been originally described in *Xenopus tropicalis* as

a gene controlling head development, however, its roles in specific developmental processes and the underlying signaling mechanisms remained uncharacterized (Kenwrick et al., 2004). In *Xenopus* gastrulae, *pnhd* is expressed in a broad ventrolateral domain in the marginal zone (Kenwrick et al., 2004; Kjolby and Harland, 2017), suggesting a role in mesoderm specification and patterning.

In this study, we evaluate a function of *pnhd* in mesoderm development. We show that *pnhd* is dynamically expressed in many tissues during *Xenopus* early development. Pnhd protein is readily secreted from frog gastrula cells and mammalian tissue culture cells. We also show that Pnhd is both necessary and sufficient for the activation of many mesoderm-specific genes. This functional activity of Pnhd required both FGF and Nodal signaling and has been manifested by the phosphorylation of Erk1. These observations lead us to propose that Pnhd is a secreted factor that controls mesoderm formation in an FGF-receptor-dependent manner.

RESULTS

Pnhd is a secreted signaling protein that modulates axial development

The pnhd gene encodes a conserved protein containing three cystine knot (CK) motifs (Avsian-Kretchmer and Hsueh, 2004; Imai et al., 2012; Isaacs, 1995). There are no other identifiable protein domains. The CK is a common feature of many extracellular proteins and has been proposed to stabilize

protein tertiary structure via disulfide bonds (Roch and Sherwood, 2014). Pnhd is present in many animals, from insects to amniotes. Sequence alignment shows the conservation of the protein throughout all three CK domains (**Fig. S1**). The CKs of Pnhd significantly deviate from those of other molecules (**Fig. 1A**), indicating that it belongs to a new class of proteins with yet uncharacterized signaling properties.

The presence of the highly hydrophobic N-terminal 22-amino-acid stretch in the deduced Pnhd protein sequence suggested a candidate signal peptide. We therefore examined whether the product of *pnhd* is secreted from the embryonic cells. To accomplish this, RNA encoding Flag-tagged Pnhd was microinjected into *Xenopus* embryos, the embryos were dissociated into single cells at the beginning of gastrulation, and the medium conditioned by the dissociated cells for three hours was examined by immunoblotting (**Fig. 1B**). Pnhd protein was predominantly found in the conditioned medium, supporting the hypothesis that it is secreted into the extracellular space. Immunoblotting revealed two bands migrating at approximately 39 and 42 kDa positions. The ratio of the upper and lower band intensities was variable, suggesting that the protein undergoes posttranslational modifications such as glycosylation. These observations have been confirmed in transfected HEK293T cells (**Fig. S2, Fig. 1C**). Full-length Pnhd protein was found largely in the medium conditioned by the transfected HEK293T cells, whereas the Pnhd construct lacking the signal peptide remained in the cell lysates (**Fig. 1C**). We estimate that at least 70-90 % of Pnhd is secreted, whereas 10-30 % is associated with the cell pellet fraction.

We next evaluated the embryonic phenotype caused by *pnhd* RNA injected into *Xenopus* early blastomeres. At tailbud stages, embryos expressing *pnhd* RNA consistently developed enlarged trunk and tail, but contained reduced or no head structures, as compared to uninjected siblings **(Fig. 1D**). We conclude that Pnhd is a secreted protein that can modulate head and axis formation in *Xenopus* embryos.

Pnhd is dynamically expressed in the early embryo

Previous reports indicate that *pnhd* RNA is enriched in the marginal zone at the onset of gastrulation (Kenwrick et al., 2004; Kjolby and Harland, 2017). To gain further insights into Pnhd function, we carried out whole mount *in situ* hybridization with embryos taken at different developmental stages. At the onset of gastrulation, *Pnhd* transcripts were detected both in the mesoderm and vegetal endoderm (**Fig. 2A-D**). Notably, *pnhd* RNA was excluded from the dorsal midline (**Fig. 2A, D, E**) as reported for many Wnt and FGF target genes (Kjolby et al., 2019). Additionally, we observed strong bilateral expression domains in the anterior neuroectoderm and weaker staining in lateral plate mesoderm at stages 13-14 (**Fig. 2F, G**), consistent with previous studies (Bae et al., 2014; Plouhinec et al., 2014). The neural plate domain appeared to correspond to the future midbrain-hindbrain boundary (MHB). At later stages, *pnhd* RNA was also enriched in the anterior preplacodal ectoderm, the dorsal neural tube and its boundary (**Fig. 2H**), and the presumptive tailbud area demarcated by the chordoneural hinge (**Fig. 2I**). At

stage 25, *pnhd* transcripts were evident at the MHB **(Fig. 2J-M),** along the dorsal midline and in the dorsal fin **(Fig. 2J, M-P).**

The identified predominant *pnhd* expression domains correspond to regions with high levels of FGF and Wnt signaling and suggest functions in the mesoderm, neural tissue, neural crest and placodes, and the dorsal fin.

Pnhd induces mesodermal markers in animal pole explants

The morphological phenotype of embryos injected with *pnhd* RNA is consistent with enhanced ventroposterior development. Pnhd expression in the ventrolateral marginal zone suggests that it may participate in mesoderm formation. We therefore assessed whether *pnhd* can induce mesoderm in animal pole ectoderm, a tissue lacking mesodermal gene expression. Whereas uninjected animal cap explants retained their spherical shape at stage 12, the explants isolated from embryos injected with *pnhd* RNA have visibly elongated (**Fig. 3A-C)**. Notably, explant elongation frequently accompanies mesoderm induction, mimicking convergent extension movements during gastrulation (Howard and Smith, 1993).

Indeed, RT-PCR demonstrated the upregulation of several mesodermal markers, including *tbxt/brachyury* (Smith et al., 1991), *wnt8a* (Christian et al., 1991) and *vegt* (Gentsch et al., 2013; Zhang et al., 1998), indicating that Pnhd can induce mesodermal progenitor fates (**Fig. 3D**). However, other markers, including the dorsal mesoderm markers *nodal3* (Smith et al., 1995) and *gsc*

(Cho et al., 1991), were not induced by Pnhd, demonstrating target selectivity. To ensure that the tag does not affect Pnhd biological activity, we used RT-qPCR to confirm that Flag-Pnhd induced *tbxt* to the same degree as the original untagged construct (**Fig. 3E)**. The mutant lacking the signal peptide was significantly less active than Pnhd (**Fig. 3E),** indicating that Pnhd secretion is critical for its function.

To unequivocally establish that Pnhd functions in the extracellular space, we tested Pnhd-Flag protein that was affinity-purified from the medium conditioned by transfected HEK293T cells. When added to ectoderm explants, the purified protein induced *tbxt* in a dose-dependent manner (**Fig. 3F**). These observations indicate that Pnhd is a new mesoderm-inducing factor that exerts its biological effects in the extracellular space.

RNA sequencing defines candidate transcriptional targets of Pnhd

An unbiased transcriptome-wide approach has been taken to identify the genes differentially regulated by Pnhd RNA in ectoderm cells (**Fig. 4A**, **Table 1**). Gene Set Enrichment Analysis (GSEA) revealed strong enrichment of mesoderm-specific markers among the top 100 upregulated genes. No specific trend was observed for the downregulated genes (data not shown). Highly ranked among the upregulated genes were known FGF and Wnt targets, including *tbxt, cdx4, hoxd1, wnt8a,* and *msgn1* (**Fig. 4B, C**) (Branney et al., 2009; Chung et al., 2004; Ding et al., 2018; Kjolby and Harland, 2017;

Nakamura et al., 2016) that have been validated by RT-qPCR (**Fig. 4D**). These genes are known to be expressed in the marginal zone, and most of them are excluded from the organizer region at the onset of gastrulation (Kjolby et al., 2019; Nakamura et al., 2016). By contrast, other mesodermal genes, such as the dorsal markers *nodal*, *gsc, or noggin,* and the ventral mesoderm (blood) markers *szl, bambi* and *ventx1.2,* have not been significantly changed, indicating that only a subset of ventroposterior mesodermal genes is sensitive to *pnhd*. These findings suggest that Pnhd is involved in paraxial mesoderm formation.

For loss-of-function analysis, two morpholino oligonucleotides (MOs) have been designed and validated in separate experiments, verifying their efficiency and specificity. Pnhd MO^{atg} efficiently blocked Pnhd RNA translation, whereas the splicing-blocking MO (Pnhd MO^{sp}) with an unrelated sequence interfered with endogenous Pnhd transcript splicing (**Fig. S3A, B**). Both MOs caused the 'pinhead' phenotype, i. e. deficiency in head structures (**Fig. S3C-E**). Importantly, the defect caused by Pnhd MO^{sp} has been rescued by Pnhd RNA (**Fig. S3F, G**).

RNA sequencing revealed putative Pnhd targets that were downregulated in marginal zone cells depleted of Pnhd. The results from the gain-of-function and the loss-of-function studies were combined to determine consensus gene targets. We found a total of 71 *pnhd* 'signature' target genes, defined as the genes upregulated in ectoderm explants by Pnhd RNA and downregulated in the marginal zone by Pnhd MO^{sp} (**Fig. 5A, Table 2**). To confirm the

requirement of *Pnhd* in mesoderm formation, selected candidate gene targets from RNA sequencing data were validated by whole mount *in situ* hybridization (WISH). Both *cdx4 and wnt8* transcripts were upregulated by Pnhd RNA overexpression and downregulated in the cells depleted of Pnhd (**Fig. 5B-F and Fig. S4A-E**). RT-qPCR further confirmed the downregulation of *cdx4, hoxd1, tbxt, msgn1* and *wnt8* transcripts in the marginal zone after *pnhd* depletion, although *tbxt* decreased only mildly, possibly because this gene is controlled by multiple signaling pathways, and the ventral marker *admp2* was unaffected (**Fig. S4F-H**).

At later stages, WISH analysis has demonstrated the disrupted and reduced expression of *myod* in *pnhd*-depleted embryos indicating abnormal somite segmentation (**Fig. S5A, B)**. The *chordin* domain appeared narrower as compared to uninjected embryos (**Fig. S5E, F)**. In contrast, the blood marker *α-globin* has not been significantly changed (**Fig. S5C, D)**.

Taken together, our gain- and loss-of-function experiments show that Pnhd signaling is involved in mesodermal fate specification during gastrulation.

Pnhd signaling depends on the FGF pathway

Since Pnhd target genes are similar to the ones activated by the FGF and Wnt pathways (Kjolby et al., 2019), we assessed whether these pathways play a role in Pnhd signaling. Importantly, we observed that *pnhd* transcription is induced in ectodermal cells by FGF and Wnt proteins (**Fig.**

S6A-C), as reported by earlier studies (Branney et al., 2009; Chung et al., 2004; Ding et al., 2018; Kjolby and Harland, 2017; Nakamura et al., 2016).

FGF proteins are known to play key roles in mesoderm development by activating tyrosine kinase receptors (FGFRs), the Akt protein kinase and extracellular signal-regulated kinases (Erk, also known as mitogen-activated protein kinase, MAPK)(Christen and Slack, 1999; Dubrulle and Pourquie, 2004; Manning and Toker, 2017; Ornitz and Itoh, 2015). To interfere with the FGF pathway we used SU5402, a pharmacological inhibitor of FGF receptor activity (Mohammadi et al., 1997)**,** a dominant negative form of FGFR1 that forms nonfunctional dimers with wild-type receptors (Amaya et al., 1991), and secreted inhibitory forms of FGF receptors (Marics et al., 2002)**.** Pnhd failed to activate *tbxt* and *cdx4* in the presence of SU5402 (**Fig. 6A**). Similarly, Pnhd activity was compromised by dominant interfering FGFR constructs (**Fig. 6B).**

To inhibit Wnt signaling, we used Dkk1 that physically associates with and inhibits the signaling through the Wnt coreceptor LRP5/6 (Bafico et al., 2001; Mao et al., 2001; Semenov et al., 2001). As expected**,** Dkk1 inhibited Wnt-dependent activation of gene targets (**Fig. 6C).** Notably, Dkk1 did not suppress the response to Pnhd (**Fig. 6C)**, indicating that Pnhd signaling does not require Wnt proteins. Consistent with this interpretation, the headless phenotype of Pnhd RNA-injected embryos has been rescued by inhibiting FGF signaling with DN-FGFR4-Fc (**Fig. S7**). These studies suggest that the stimulation of target genes by Pnhd requires FGF but not Wnt activity.

Erk1 but not Akt may mediate Pnhd effects on transcription

To further investigate the pathways that are modulated by Pnhd, we examined the abundance and the phosphorylation status of the common cytoplasmic signaling mediators in *pnhd*-expressing cells. The direct comparison of FGF and Pnhd effects on early ectoderm confirmed that, unlike FGF, Pnhd does not activate Erk1 in the early explants that are isolated at stage 8 and cultured until stage 10 **(Fig. 7A, B).** Interestingly, in the same explants, we found that Pnhd, but not FGF, led to the pronounced inhibition of Akt, a kinase implicated in many pathways including receptor tyrosine kinase signaling (Manning and Toker, 2017). By contrast, β-catenin levels did not change **(Fig. 7B**). The negative effect of Pnhd on Akt was reproducible and stage-dependent, it was less pronounced at the end of gastrulation and correlated with Erk phosphorylation **(Fig. 7C, D).**

To assess the importance of the observed phospho-Akt downregulation for Pnhd-dependent Erk activation, we modulated the function of PI3 kinase, an upstream activator of Akt (Manning and Toker, 2017). Neither stimulation of Akt by the constitutively active PI3K (p110CAAX) (Carballada et al., 2001) nor its inhibition by the phosphatase PTEN influenced the ability of Pnhd to stimulate Erk phosphorylation (**Fig. 7D, Fig. S8**). Although Akt does not appear to mediate Pnhd signaling to Erk in these experiments, it may function in a parallel pathway that affects mesoderm development independently of Erk (Carballada et al., 2001; Dubrulle and Pourquie, 2004).

By contrast, overexpressed Pnhd caused robust phospho-Erk1 accumulation at gastrula stages (**Fig. 7C-E**). Of note, the Pnhd construct lacking the signal peptide failed to activate Erk1 (**Fig. 7E**). Conversely, phospho-Erk1 level decreased in Pnhd-depleted embryos, similar to the effect of DN-FGFR1 (**Fig. 7F**). No significant changes in β-catenin levels or Smad1 phosphorylation were detected in Pnhd-depleted embryos, supporting specificity (**Fig. 7F**). These observations are consistent with the idea that Pnhd promotes mesoderm formation via the FGF- and Erk-dependent pathway.

We next evaluated whether Pnhd signaling is affected by the Nodal/Activin pathway. Notably, the stimulation of animal cap explants with Pnhd enhanced Activin-dependent Smad2 phosphorylation, indicating cross-talk (**Fig. 7G**). On its own, Pnhd did not change phospho-Smad2 levels (data not shown). Notably, SB505124, an inhibitor of Nodal/Activin receptor signaling (DaCosta Byfield et al., 2004), interfered with Pnhd-dependent target gene activation and explant elongation (**Fig. S9**). These observations indicate that both FGF and Nodal pathways contribute to the ability of Pnhd to activate mesodermal gene targets.

Pnhd expression in the marginal zone is essential for mesoderm formation during gastrulation

To get insights into the developmental stage at which Pnhd operates, we examined whether the Pnhd effect depends on the time of animal cap

isolation **(Fig. 8A)**. When the explants were isolated at stage 10 and cultured to stage 12, they robustly elongated in response to *pnhd* RNA (**Fig. S10**). However, the response was undetectable in the explants prepared at stage 8 (**Fig. S10**). Moreover, the explants isolated at stage 10 rather than the ones isolated at stage 8 revealed preferential phosphorylation of Erk1 (**Fig. 8B**) and selective activation of Pnhd gene targets (**Fig. 8C**). The only difference between the two groups of explants containing Pnhd is the *time of their contact with the inducing tissue,* i. e. adjacent mesendoderm. Therefore, between stage 8 and stage 10, the explanted ectoderm must have received additional signals from the marginal zone (Sokol, 1993). Thus, Pnhd induces *cdx4* and *tbxt* synergistically with these additional signals and this may involve the Nodal or/and the FGF pathway, as predicted by our inhibitor studies.

We next studied whether Pnhd is required for mesoderm formation in response to the endogenous inducing signals in animal-vegetal conjugates. Mesoderm-specific gene activation has been suppressed in *pnhd*-depleted conjugates as compared to wild-type controls (**Fig. 8D, E**). This result supports our model that Pnhd functions in mesoderm specification in response to initial mesoderm-inducing signals. We also assessed whether Pnhd is required for mesoderm induction by FGF. FGF-dependent induction of *cdx4 and tbxt* was strongly inhibited in Pnhd morphants (**Fig. S11**), consistent with the positive feedback between Pnhd and FGF.

Based on these findings, we propose that Pnhd is activated in the marginal zone by early vegetal inducing signals and, in turn, functions in the marginal zone by triggering multiple mesodermal markers (see **Fig. 8D**).

DISCUSSION

This study identifies *pnhd* as a secreted regulator of mesoderm formation during *Xenopus* gastrulation. Many genes induced by Pnhd are FGF-dependent markers and modulators of posterior mesoderm, such as *tbxt, msgn1* or *cdx4*. By contrast, many dorsal markers, including *nodal*, *gsc, noggin,* and ventral genes, such as *szl, bambi* and *ventx1.2,* were not affected in Pnhd-depleted marginal zone explants based on our RNA seq analysis. Being produced in the marginal zone during gastrulation, *pnhd* appears to predominantly affect presumptive somitic mesoderm. Nevertheless, the analysis of single cell transcriptome data using the SPRING tool (Briggs et al., 2018) indicates that *pnhd* itself is not transcribed in the *cdx4-, hoxd1- or msgn1*-expressing cells (data not shown), suggesting that it modulates target genes in the paracrine rather than autocrine manner. The activation of caudal-related (*cdx*) genes, *tbx* genes (*tbxt* and *vegt*), and posteriorly expressed *hox* genes is characteristic of the tail organizer (De Robertis and Kuroda, 2004; Harland and Gerhart, 1997; Niehrs, 2004) and provides an explanation for the headless phenotype of Pnhd-expressing embryos. We note that this phenotype is consistent with the increased posteriorizing activity of FGF (Cox and Hemmati-Brivanlou, 1995; Lamb and Harland, 1995) and can be rescued by inhibiting FGF signaling (**Fig. S7**). Our marker analysis at later stages

support the view that Pnhd primarily affects paraxial mesoderm, as evident by the disrupted segmentation of *myod*-positive somites at later stages and the lack of effect on α*-globin* (**Fig. S5**). The narrow *chordin* domain in *pnhd*-depleted embryos leaves open the possibility that *pnhd* might have a role in notochord development. Nevertheless, the late developmental defects of *pnhd* morphants are modest, suggesting that other pathways maintain mesoderm when *pnhd* is no longer expressed. This conclusion reiterates the existence of multiple signaling pathways operating during mesoderm specification (Gentsch et al., 2013; Kimelman, 2006; Loose and Patient, 2004; Morley et al., 2009).

Many putative Pnhd target genes are expressed in the ventrolateral marginal zone during gastrulation and largely overlap with FGF and Wnt targets (Branney et al., 2009; Chung et al., 2004; Ding et al., 2018; Kjolby and Harland, 2017; Nakamura et al., 2016). The DNA regulatory sequences of these target genes include T-cell factor (TCF) and Ets DNA-binding sites that are engaged and contribute to the transcriptional regulation (Kjolby et al., 2019). Consistent with the cross-talk with the FGF pathway, Pnhd-mediated target gene transcription strongly correlates with Erk1 phosphorylation. Whereas PI3K-Akt signaling does not modulate Erk activation by Pnhd, it is may be involved in a parallel pathway leading to mesoderm development (Carballada et al., 2001; Dubrulle and Pourquie, 2004). We note that Pnhd functions differently from canonical Wnt ligands, because the cell response to Pnhd cannot be blocked by the Wnt antagonist Dkk1. *Pnhd RNA does not* trigger secondary axis formation or activate the direct Wnt target *nodal3*.

Also, there is no decrease of the level of β-catenin, a common Wnt component.

Our observations contrast those of Kenwrick et al., who observed enlarged anterior structures in *X. tropicalis* embryos injected with *pnhd* RNA (Kenwrick et al., 2004). The study hypothesized that the 'pinhead' phenotype of the morphants is due to the inhibitory effect of Pnhd on the Wnt pathway. Although *pnhd*-overexpressing embryos sometimes appear anteriorized at tailbud stages due to the developmental delay, we find that Wnt target genes are commonly stimulated rather than repressed by Pnhd. Two other studies proposed that Pnhd inhibits (Imai et al., 2012) or promotes (Yan et al., 2019) the activity of Admp, a BMP-related protein (Dosch and Niehrs, 2000; Joubin and Stern, 1999; Moos et al., 1995). Whereas both *Xenopus* Admp proteins stimulate ventral mesoderm formation characterized by active Smad1 (Kumano et al., 2006), *pnhd* morphants had no changes in Smad1 phosphorylation. Thus, crosstalk of Pnhd with distinct signaling pathways remains to be investigated in more detail in future studies.

We have demonstrated that Pnhd is essential for the response of embryonic cells to exogenous FGF and endogenous vegetal inducing signals. Conversely, blocking FGF and Nodal signaling interferes with Pnhd-mediated activation of mesodermal genes. Notably, Nodal/Activin signaling has been shown to require the FGF pathway in *Xenopus* embryos (Cornell et al., 1995; LaBonne and Whitman, 1994). The interdependence of *pnhd,* FGF and Nodal signaling highlights the positive regulatory feedback during posterior

mesoderm development and, possibly, later at the MHB and other sites of *pnhd* expression.

Whereas the *pnhd* gene has been conserved in many animals from insects to reptiles and birds, it is absent in mammals, suggesting differences in mesoderm specification. It is currently unknown how the Pnhd signal is transmitted inside the cell. Presumably, the cystine-knot motif of Pnhd interacts with a receptor at the cell surface. Whereas our experiments did not detect the association with FGF receptors (data not shown), it is possible that Pnhd forms a complex with a heparan sulfate proteoglycan that functions as FGF coreceptor (Lin, 2004; Ornitz, 2000). Alternatively, Pnhd may act by binding to molecules in the extracellular space, as shown for other pleiotropic modulators containing the cystine-knot motif, such as Cerberus or Wise (Imai et al., 2012; Lintern et al., 2009; Piccolo et al., 1999). Future analysis of Pnhd interactions with various signaling proteins is warranted to elucidate the mechanism underlying its effects on embryonic mesoderm.

METHODS

Plasmids, in vitro RNA synthesis and morpholino oligonucleotides (MOs).

pCS2-Pnhd, pCS2-Flag-Pnhd, pCS2-Flag-PnhdSP, pCS2-Pnhd-Flag and pCS2-HA-Pnhd plasmids have been generated by PCR from the *X. laevis* DNA clone for *pnhd.L* (accession number NM_001127751) obtained from Dharmacon. *pnhd.L* fragment was subcloned into the Bgl2/BamH1 sites of

pXT7 to produce pXT7-Pnhd. pCS2-mFGF8-HA was generated by sub-cloning BamH1-Cla1 DNA fragment from pBSSK-mFGF8 variant I (Crossley and Martin, 1995) into pCS2-HA. pCS2-PTEN-HA was from Jeff Wrana (Shnitsar et al., 2015), constitutively active pI3K (p110CAAX) in pCS2 (Carballada et al., 2001) was from Chenbei Chang, pBSSK-chordin was from Eddy De Robertis. Plasmids containing α-*globin, myod, wnt8a* and *cdx4* anti-sense probes have been generated by PCR. Details of cloning are available upon request.

Capped mRNAs were synthesized using mMessage mMachine kit (Ambion, Austin, TX). In addition to Pnhd and FGF8 plasmids, the following plasmids have been used: pCS2-hDkk1 (Krupnik et al., 1999), pSP64T-Wnt3a (Wolda et al., 1993), pXT7-GFP-C1, pCS2-nucβGal, pSP64T-Wnt8 (Sokol et al., 1991), DN-FGFR1 (Amaya et al., 1991), and the secreted inhibitory forms of FGFR1 and 4 (FGFR1-Fc and FGFR4-Fc) (Marics et al., 2002). pCS2-HA-XVangl2 construct has been described (Ossipova et al., 2015). The following MOs were purchased from Gene Tools (Philomath, OR): Pnhd MO^{atg} (translation-blocking), 5'-A CAA GAA AAG ATG TTC CAT GTC TG-3'; Pnhd MO^{sp} (splicing-blocking), 5'-CCTGTTCATCACGCTACCATCTAAA-3'; control MO (CoMO), 5'-GCTTCAGCTAGTGACACATGCAT-3'.

Xenopus embryo culture and microinjections, explants, secreted protein production and treatment.

In vitro fertilization and culture of *Xenopus laevis* embryos were carried out as previously described (Dollar et al., 2005). Staging was according to

Nieuwkoop and Faber (Nieuwkoop and Faber, 1967). For microinjections, 2-4-cell embryos were transferred into 2-3 % Ficoll in 0.5x Marc's Modified Ringer's (MMR) solution (50 mM NaCl, 1 mM KCl, 1 mM $CaCl_2$, 0.5 mM $MgCl_2$, 2.5 mM HEPES pH 7.4) (Peng, 1991) and 5-10 nl of mRNA or MO solution were injected into one or more blastomeres. Amounts of injected mRNA per embryo have been optimized in preliminary dose-response experiments (data not shown) and are indicated in figure legends. For animal cap experiments, both blastomeres at the 2-cell stage were injected in the animal pole region.

Ectoderm (animal caps), vegetal or marginal zone explants were prepared at stages 8 to 11, and cultured in 0.6xMMR until the indicated time for morphological observations, RNA extraction or immunoblot analysis. Stimulation of ectoderm explants with 50 ng/ml of *Xenopus* recombinant bFGF or 1 ng/ml of human Activin βA has been performed as described (Itoh and Sokol, 1994). For stimulation with Pnhd, stage 10 ectoderm explants were cultured with 1.5 µg/ml or 6.5 µg/ml of Flag-Pnhd in 0.6xMMR until stage 11 or stage 14. Animal-vegetal conjugates were prepared right after dissection and cultured until stage 11 for RNA extraction.

Secreted proteins were produced after dissociating animal pole cells in Ca/Mg-free medium, culturing them for 2-3 hrs and collecting the supernatant for analysis. SU5402 (Calbiochem), a pharmacological inhibitor of FGF signaling, and type I TGFβ receptor inhibitor SB505124 (Sigma) have been

prepared as 10 mM stock solutions in DMSO and used at a final concentration of 100 µM.

Cell culture and transfection

Human embryonic kidney 293T cells were maintained in DMEM (Corning) with 10 % fetal bovine serum (Gemini) and penicillin/streptomycin (Sigma). Cells growing at 70 % confluence were transiently transfected using linear polyethylenimine (M.W. 25,000, Polysciences) as described (Ossipova et al., 2009). Briefly, each 35-mm dish with cells received 1.5 µg of pCS2 plasmids encoding Flag-Pnhd or Flag-GFP as a control. Vector DNA (pCS2) was added to the plasmid DNA mixture to reach the total DNA amount of 3 µg. Cell supernatants and lysates were collected 24-48 hrs after transfection. The Flag-Pnhd protein was produced from 50 ml culture of transiently transfected HEK293T cells (Bonopus, NJ) and was stored frozen at -80^{o} C. Flag-Pnhd protein levels were estimated by comparison with known amounts of BSA on a Coomassie-stained gel.

RNA sequencing

Pnhd-expressing (1.5 ng) and control uninjected animal pole cells were cultured until stage 11. For pnhd knockdown, 10 ng of *pnhd* MO^{atg} or 40 ng of *pnhd* MO^{sp} were injected two to four times into marginal zone of four-cell embryos. RNA was extracted from marginal zone explants at stage 10.5 or ectoderm explants at stage 11-11.5 using RNeasy kit (Qiagen), cDNA library preparation and paired-end 150 bp sequencing were performed by Novogene (Sacramento, CA) using Illumina HiSeq2000 analyzers. The raw reads

(FASTQ files) were filtered to remove reads containing adapters or reads of low quality. The sequences were mapped to the *Xenopus* genome version XL-9.1_v1.8.3.2 available at http://www.xenbase.org/other/static/ftpDatafiles.jsp using the software hisat2 (Kim et al., 2015). The Total Mapped Reads were larger than 73 % for all samples and the Multiple Mapped Reads were lower than 9%, which is within the generally accepted limits of higher than 70 % and lower than 10 %, respectively. The files were sorted using the Samtools package (http://www.htslib.org/doc/samtools-1.2.html). The sequences were counted using the HTSeq package (Anders et al., 2015). The differentially expressed genes (DEGs) were detected using DESeq (Anders and Huber, 2010) with the two-fold change cutoff. The p-value estimation was based on the negative binomial distribution, using the Benjamini-Hochberg estimation model with the adjusted $p < 0.05$. The heatmap and the volcano plots were generated using the publicly available software BioJupies (Torre et al., 2018). Differentially expressed genes (DEGs) have been evaluated by the Gene Set Enrichment Analysis (GSEA) software (Subramanian et al., 2005). The RNA-seq data reported in this paper have been deposited in the Gene Expression Omnibus (GEO, www.ncbi.nlm.nih.gov/geo) database (accession no. GSE143795). Pnhd-induced DEGs have been assessed from four separate RNA sequencing experiments using independent samples.

Ectoderm explants, RT-PCR and qRT-PCR

RNA was extracted from a group of 3-5 mixed embryos, 6-10 marginal zone or 10-30 animal pole explants, using the RNeasy kit (Qiagen). For RT-PCR,

cDNA was made from 1-2 µg of total RNA using the first strand cDNA kit (Invitrogen) or iScript (Bio-Rad) according to the manufacturer's instructions. PCR with Taq polymerase was carried out based on standard protocols. For RT-qPCR, the reactions were amplified using a CFX96 light cycler (Bio-Rad) with Universal SYBR Green Supermix (Bio-Rad). Primer sequences used for RT-PCR and RT-qPCR have been described (Ossipova and Sokol, 2011) or shown in **Table 3**. The reaction mixture consisted of 1X Power SYBR Green PCR Master Mix, 0.3 µM primers, and 1 µl of cDNA in a total volume of 10 µl. The cycling conditions for RT-qPCR used were as following: 1. incubation at 95°C for 3 min; 2. activation at 95°C for 0.10 min; 3. 60° for 0.30 min; 4. 39 cycles to step 2; 5. 65°C for 0.05 min and 95°C for 0.5 min. The ΔΔCT method was used to quantify the results. All samples were normalized to control uninjected embryos or explants. Transcripts for *elongation factor 1a1 (ef1a1*) were used for normalization. Data are representative of two to three independent experiments and shown as means +/- standard errors. Statistical significance was assessed by the Student's t-test.

Wholemount in situ hybridization

Wholemount in situ hybridization (WISH) and XGAL staining were carried out as described (Harland, 1991), except when RedGAL substrate was used instead of XGAL. Diogoxigenin-rUTP–labeled RNA probes were prepared by in vitro transcription of linearized *pnhd.L*, *chordin, α-globin, myod*, *cdx4* and *wnt8a DNA* templates with T7 or SP6 RNA polymerases and the RNA labeling mix containing digoxigenin-rUTP (Roche). nuclear *β-galactosidase (β-gal)* RNA (50 pg) was a lineage tracer. For the sense probe, the same *pnhd*

construct was linearized with Bgl2 and transcribed with Sp6 polymerase. A second anti-sense *pnhd* probe was prepared with linearizing the same plasmid with EcoRV. For *pnhd.L*, the same expression pattern after *in situ* hybridization was obtained using two different anti-sense RNA probes. *In situ* stained embryos were embedded in coldwater fish gelatin-sucrose mixture to prepare 25 µm cryosections using Leica CM3050 cryostat (Ossipova and Sokol, 2020). Images were digitally acquired on the Zeiss Axio Imager microscope. All data are representative of two to three independent experiments.

Immunoprecipitation and immunoblot analysis

For immunoprecipitation, cells transfected for 24 hours were lysed in IP buffer (10 mM HEPES pH 7.4, 150 mM NaCl, 1 mM EGTA, 1 mM $MgCl_2$, 1% Triton X-100, 1 mM Na_3VO_4, 10 mM NaF, 25 mM β-glycerol phosphate), containing protease inhibitor cocktail (complete Mini EDTA-free, Roche). After centrifugation for 5 min at 16,000 g, the supernatant was incubated with anti-FLAG agarose beads (Sigma) at 4°C for 2-3 hours. The beads were washed three times with IP buffer and boiled in the SDS-PAGE sample buffer. Immunoblot analysis was carried out essentially as described (Itoh et al., 2005). Briefly, 5 embryos at stage 10.5 were homogenized in 75 µl of the lysis buffer (50 mM Tris-HCl pH 7.6, 50 mM NaCl, 1 mM EDTA, 1% Triton X-100, 10 mM NaF, 1 mM Na_3VO_4, 25 mM β-glycerol phosphate, 1 mM PMSF). After centrifugation for 3 min at 16000 g, the supernatant was subjected to SDS-PAGE and western blot analysis following standard protocols. The following primary antibodies were used: mouse anti-FLAG (M2, Sigma), rabbit

anti-HA (Bethyl Labs), rabbit anti-pErk1 (Phospho-p44/42, T202/Y204, Cell Signaling), rabbit anti-Erk1 (K23, Santa Cruz), anti-pSmad1/5 S463/465 (Cell signaling) and anti-Smad1 (Invitrogen Life Technologies), rabbit anti-pSmad2 (Cell Signaling), rabbit anti-pAkt (S473, Cell Signaling), anti-Akt (Cell Signaling), and mouse anti-β-catenin (Santa Cruz). The detection was carried out by enhanced chemiluminescence as described (Itoh et al., 2005), using the ChemiDoc MP imager (BioRad). Every immunoblotting result has been repeated 3-12 times.

Acknowledgement. We thank Rohan Bareja, Olivier Elemento and the Mount Sinai Genomics Core Facility for help with RNAseq analysis at the early stages of this project, Phil Soriano and David Kimelman for FGF plasmids, Eddy De Robertis for *chordin* plasmid, Jeff Wrana for PTEN and Chenbei Chang for pI3 kinase plasmids. We are grateful to Kety Giannetti for confirming PnhdMO^{sp} efficiency by RT-PCR. We thank Miho Matsuda for the critical reading of the manuscript and members of the Sokol laboratory for discussions. This study was supported by the NICHD grant HD092990 to S. S.

References

Amaya, E., Musci, T. J. and Kirschner, M. W. (1991). Expression of a dominant negative mutant of the FGF receptor disrupts mesoderm formation in *Xenopus* embryos. *Cell* **66**, 257-270.

Anders, S. and Huber, W. (2010). Differential expression analysis for sequence count data. *Genome Biol* **11**, R106.

Anders, S., Pyl, P. T. and Huber, W. (2015). HTSeq--a Python framework to work with high-throughput sequencing data. *Bioinformatics* **31**, 166-169.

Avsian-Kretchmer, O. and Hsueh, A. J. (2004). Comparative genomic analysis of the eight-membered ring cystine knot-containing bone morphogenetic protein antagonists. *Mol Endocrinol* **18**, 1-12.

Bae, C. J., Park, B. Y., Lee, Y. H., Tobias, J. W., Hong, C. S. and Saint-Jeannet, J. P. (2014). Identification of Pax3 and Zic1 targets in the developing neural crest. *Dev Biol* **386**, 473-483.

Bafico, A., Liu, G., Yaniv, A., Gazit, A. and Aaronson, S. A. (2001). Novel mechanism of Wnt signalling inhibition mediated by Dickkopf-1 interaction with LRP6/Arrow. *Nat Cell Biol* **3**, 683-686.

Branney, P. A., Faas, L., Steane, S. E., Pownall, M. E. and Isaacs, H. V. (2009). Characterisation of the fibroblast growth factor dependent transcriptome in early development. *PLoS One* **4**, e4951.

Briggs, J. A., Weinreb, C., Wagner, D. E., Megason, S., Peshkin, L., Kirschner, M. W. and Klein, A. M. (2018). The dynamics of gene expression in vertebrate embryogenesis at single-cell resolution. *Science* **360**.

Carballada, R., Yasuo, H. and Lemaire, P. (2001). Phosphatidylinositol-3 kinase acts in parallel to the ERK MAP kinase in the FGF pathway during Xenopus mesoderm induction. *Development* **128**, 35-44.

Cho, K. W., Blumberg, B., Steinbeisser, H. and De Robertis, E. M. (1991). Molecular nature of Spemann's organizer: the role of the Xenopus homeobox gene goosecoid. *Cell* **67**, 1111-1120.

Christen, B. and Slack, J. M. (1999). Spatial response to fibroblast growth factor signalling in Xenopus embryos. *Development* **126**, 119-125.

Christian, J. L., McMahon, J. A., McMahon, A. P. and Moon, R. T. (1991). Xwnt-8, a Xenopus Wnt-1/int-1-related gene responsive to mesoderm-inducing growth factors, may play a role in ventral mesodermal patterning during embryogenesis. *Development* **111**, 1045-1055.

Chung, H. A., Hyodo-Miura, J., Kitayama, A., Terasaka, C., Nagamune, T. and Ueno, N. (2004). Screening of FGF target genes in Xenopus by microarray: temporal dissection of the signalling pathway using a chemical inhibitor. *Genes Cells* **9**, 749-761.

Cornell, R. A., Musci, T. J. and Kimelman, D. (1995). FGF is a prospective competence factor for early activin-type signals in Xenopus mesoderm induction. *Development* **121**, 2429-2437.

Cox, W. G. and Hemmati-Brivanlou, A. (1995). Caudalization of neural fate by tissue recombination and bFGF. *Development* **121**, 4349-4358.

Crossley, P. H. and Martin, G. R. (1995). The mouse Fgf8 gene encodes a family of polypeptides and is expressed in regions that direct outgrowth and patterning in the developing embryo. *Development* **121**, 439-451.

DaCosta Byfield, S., Major, C., Laping, N. J. and Roberts, A. B. (2004). SB-505124 is a selective inhibitor of transforming growth factor-beta type I receptors ALK4, ALK5, and ALK7. *Mol Pharmacol* **65**, 744-752.
De Robertis, E. M. and Kuroda, H. (2004). Dorsal-ventral patterning and neural induction in Xenopus embryos. *Annu Rev Cell Dev Biol* **20**, 285-308.
Ding, Y., Colozza, G., Sosa, E. A., Moriyama, Y., Rundle, S., Salwinski, L. and De Robertis, E. M. (2018). Bighead is a Wnt antagonist secreted by the Xenopus Spemann organizer that promotes Lrp6 endocytosis. *Proc Natl Acad Sci U S A* **115**, E9135-E9144.
Dollar, G. L., Weber, U., Mlodzik, M. and Sokol, S. Y. (2005). Regulation of Lethal giant larvae by Dishevelled. *Nature* **437**, 1376-1380.
Dosch, R. and Niehrs, C. (2000). Requirement for anti-dorsalizing morphogenetic protein in organizer patterning. *Mech Dev* **90**, 195-203.
Dubrulle, J. and Pourquie, O. (2004). fgf8 mRNA decay establishes a gradient that couples axial elongation to patterning in the vertebrate embryo. *Nature* **427**, 419-422.
Gentsch, G. E., Owens, N. D., Martin, S. R., Piccinelli, P., Faial, T., Trotter, M. W., Gilchrist, M. J. and Smith, J. C. (2013). In vivo T-box transcription factor profiling reveals joint regulation of embryonic neuromesodermal bipotency. *Cell Rep* **4**, 1185-1196.
Harland, R. and Gerhart, J. (1997). Formation and function of Spemann's organizer. *Annu. Rev. Cell Dev. Biol.* **13**, 611-667.
Harland, R. M. (1991). *In situ* hybridization: an improved whole-mount method for *Xenopus* embryos. In *Methods Cell Biol.* (ed. B. K. Kay & H. B. Peng), pp. 685-695. San Diego: Academic Press Inc.
Howard, J. E. and Smith, J. C. (1993). Analysis of gastrulation: different types of gastrulation movement are induced by different mesoderm-inducing factors in Xenopus laevis. *Mech Dev* **43**, 37-48.
Imai, K. S., Daido, Y., Kusakabe, T. G. and Satou, Y. (2012). Cis-acting transcriptional repression establishes a sharp boundary in chordate embryos. *Science* **337**, 964-967.
Isaacs, N. W. (1995). Cystine knots. *Curr Opin Struct Biol* **5**, 391-395.
Itoh, K., Brott, B. K., Bae, G. U., Ratcliffe, M. J. and Sokol, S. Y. (2005). Nuclear localization is required for Dishevelled function in Wnt/beta-catenin signaling. *J Biol* **4**, 3.
Joubin, K. and Stern, C. D. (1999). Molecular interactions continuously define the organizer during the cell movements of gastrulation. *Cell* **98**, 559-571.
Kenwrick, S., Amaya, E. and Papalopulu, N. (2004). Pilot morpholino screen in Xenopus tropicalis identifies a novel gene involved in head development. *Dev Dyn* **229**, 289-299.
Kiecker, C., Bates, T. and Bell, E. (2016). Molecular specification of germ layers in vertebrate embryos. *Cell Mol Life Sci* **73**, 923-947.
Kim, D., Langmead, B. and Salzberg, S. L. (2015). HISAT: a fast spliced aligner with low memory requirements. *Nat Methods* **12**, 357-360.
Kimelman, D. (2006). Mesoderm induction: from caps to chips. *Nat Rev Genet* **7**, 360-372.

Kjolby, R. A. S. and Harland, R. M. (2017). Genome-wide identification of Wnt/beta-catenin transcriptional targets during Xenopus gastrulation. *Dev Biol* **426**, 165-175.
Kjolby, R. A. S., Truchado-Garcia, M., Iruvanti, S. and Harland, R. M. (2019). Integration of Wnt and FGF signaling in the Xenopus gastrula at TCF and Ets binding sites shows the importance of short-range repression by TCF in patterning the marginal zone. *Development* **146**.
Krupnik, V. E., Sharp, J. D., Jiang, C., Robison, K., Chickering, T. W., Amaravadi, L., Brown, D. E., Guyot, D., Mays, G., Leiby, K., et al. (1999). Functional and structural diversity of the human Dickkopf gene family. *Gene* **238**, 301-313.
Kumano, G., Ezal, C. and Smith, W. C. (2006). ADMP2 is essential for primitive blood and heart development in Xenopus. *Dev Biol* **299**, 411-423.
LaBonne, C. and Whitman, M. (1994). Mesoderm induction by activin requires FGF-mediated intracellular signals. *Development* **120**, 463-472.
Lamb, T. M. and Harland, R. M. (1995). Fibroblast growth factor is a direct neural inducer, which combined with noggin generates anterior-posterior neural pattern. *Development* **121**, 3627-3636.
Langdon, Y. G. and Mullins, M. C. (2011). Maternal and zygotic control of zebrafish dorsoventral axial patterning. *Annu Rev Genet* **45**, 357-377.
Lin, X. (2004). Functions of heparan sulfate proteoglycans in cell signaling during development. *Development* **131**, 6009-6021.
Lintern, K. B., Guidato, S., Rowe, A., Saldanha, J. W. and Itasaki, N. (2009). Characterization of wise protein and its molecular mechanism to interact with both Wnt and BMP signals. *J Biol Chem* **284**, 23159-23168.
Loose, M. and Patient, R. (2004). A genetic regulatory network for Xenopus mesendoderm formation. *Dev Biol* **271**, 467-478.
Manning, B. D. and Toker, A. (2017). AKT/PKB Signaling: Navigating the Network. *Cell* **169**, 381-405.
Mao, B., Wu, W., Li, Y., Hoppe, D., Stannek, P., Glinka, A. and Niehrs, C. (2001). LDL-receptor-related protein 6 is a receptor for Dickkopf proteins. *Nature* **411**, 321-325.
Marics, I., Padilla, F., Guillemot, J. F., Scaal, M. and Marcelle, C. (2002). FGFR4 signaling is a necessary step in limb muscle differentiation. *Development* **129**, 4559-4569.
Mohammadi, M., McMahon, G., Sun, L., Tang, C., Hirth, P., Yeh, B. K., Hubbard, S. R. and Schlessinger, J. (1997). Structures of the tyrosine kinase domain of fibroblast growth factor receptor in complex with inhibitors. *Science* **276**, 955-960.
Moos, M., Jr., Wang, S. and Krinks, M. (1995). Anti-dorsalizing morphogenetic protein is a novel TGF-beta homolog expressed in the Spemann organizer. *Development* **121**, 4293-4301.
Morley, R. H., Lachani, K., Keefe, D., Gilchrist, M. J., Flicek, P., Smith, J. C. and Wardle, F. C. (2009). A gene regulatory network directed by zebrafish No tail accounts for its roles in mesoderm formation. *Proc Natl Acad Sci U S A* **106**, 3829-3834.

Nakamura, Y., de Paiva Alves, E., Veenstra, G. J. and Hoppler, S. (2016). Tissue- and stage-specific Wnt target gene expression is controlled subsequent to beta-catenin recruitment to cis-regulatory modules. *Development* **143**, 1914-1925.
Niehrs, C. (2004). Regionally specific induction by the Spemann-Mangold organizer. *Nat Rev Genet* **5**, 425-434.
Nieuwkoop, P. D. and Faber, J. (1967). *Normal Table of Xenopus laevis (Daudin)*. Amsterdam: North Holland.
Ornitz, D. M. (2000). FGFs, heparan sulfate and FGFRs: complex interactions essential for development. *Bioessays* **22**, 108-112.
Ornitz, D. M. and Itoh, N. (2015). The Fibroblast Growth Factor signaling pathway. *Wiley Interdiscip Rev Dev Biol* **4**, 215-266.
Ossipova, O., Chu, C. W., Fillatre, J., Brott, B. K., Itoh, K. and Sokol, S. Y. (2015). The involvement of PCP proteins in radial cell intercalations during Xenopus embryonic development. *Dev Biol* **408**, 316-327.
Ossipova, O., Ezan, J. and Sokol, S. Y. (2009). PAR-1 phosphorylates Mind bomb to promote vertebrate neurogenesis. *Dev Cell* **17**, 222-233.
Ossipova, O. and Sokol, S. Y. (2011). Neural crest specification by noncanonical Wnt signaling and PAR-1. *Development* **138**, 5441-5450.
Ossipova, O. and Sokol, S. Y. (2020). Cryosectioning and Immunostaining of Xenopus embryonic tissues. *Cold Spring Harbor Protocols* (submitted).
Peng, H. B. (1991). Xenopus laevis: Practical uses in cell and molecular biology. Solutions and protocols. *Methods Cell Biol* **36**, 657-662.
Piccolo, S., Agius, E., Leyns, L., Bhattacharyya, S., Grunz, H., Bouwmeester, T. and De Robertis, E. M. (1999). The head inducer Cerberus is a multifunctional antagonist of Nodal, BMP and Wnt signals. *Nature* **397**, 707-710.
Plouhinec, J. L., Roche, D. D., Pegoraro, C., Figueiredo, A. L., Maczkowiak, F., Brunet, L. J., Milet, C., Vert, J. P., Pollet, N., Harland, R. M., et al. (2014). Pax3 and Zic1 trigger the early neural crest gene regulatory network by the direct activation of multiple key neural crest specifiers. *Dev Biol* **386**, 461-472.
Roch, G. J. and Sherwood, N. M. (2014). Glycoprotein hormones and their receptors emerged at the origin of metazoans. *Genome Biol Evol* **6**, 1466-1479.
Rodaway, A. and Patient, R. (2001). Mesendoderm. an ancient germ layer? *Cell* **105**, 169-172.
Schohl, A. and Fagotto, F. (2002). Beta-catenin, MAPK and Smad signaling during early Xenopus development. *Development* **129**, 37-52.
Semenov, M. V., Tamai, K., Brott, B. K., Kuhl, M., Sokol, S. and He, X. (2001). Head inducer Dickkopf-1 is a ligand for Wnt coreceptor LRP6. *Curr Biol* **11**, 951-961.
Shnitsar, I., Bashkurov, M., Masson, G. R., Ogunjimi, A. A., Mosessian, S., Cabeza, E. A., Hirsch, C. L., Trcka, D., Gish, G., Jiao, J., et al. (2015). PTEN regulates cilia through Dishevelled. *Nat Commun* **6**, 8388.
Smith, J. C., Price, B. M., Green, J. B., Weigel, D. and Herrmann, B. G. (1991). Expression of a Xenopus homolog of Brachyury (T) is an immediate-early response to mesoderm induction. *Cell* **67**, 79-87.

Smith, W. C., McKendry, R., Ribisi, S., Jr. and Harland, R. M. (1995). A nodal-related gene defines a physical and functional domain within the Spemann organizer. *Cell* **82**, 37-46.

Sokol, S., Christian, J. L., Moon, R. T. and Melton, D. A. (1991). Injected Wnt RNA induces a complete body axis in *Xenopus* embryos. *Cell* **67**, 741-752.

Sokol, S. Y. (1993). Mesoderm formation in Xenopus ectodermal explants overexpressing Xwnt8: evidence for a cooperating signal reaching the animal pole by gastrulation. *Development* **118**, 1335-1342.

Subramanian, A., Tamayo, P., Mootha, V. K., Mukherjee, S., Ebert, B. L., Gillette, M. A., Paulovich, A., Pomeroy, S. L., Golub, T. R., Lander, E. S., et al. (2005). Gene set enrichment analysis: a knowledge-based approach for interpreting genome-wide expression profiles. *Proc Natl Acad Sci U S A* **102**, 15545-15550.

Torre, D., Lachmann, A. and Ma'ayan, A. (2018). BioJupies: Automated Generation of Interactive Notebooks for RNA-Seq Data Analysis in the Cloud. *Cell Syst* **7**, 556-561 e553.

Wolda, S. L., Moody, C. J. and Moon, R. T. (1993). Overlapping expression of Xwnt-3A and Xwnt-1 in neural tissue of Xenopus laevis embryos. *Dev Biol* **155**, 46-57.

Yan, Y., Ning, G., Li, L., Liu, J., Yang, S., Cao, Y. and Wang, Q. (2019). The BMP ligand Pinhead together with Admp supports the robustness of embryonic patterning. *Sci Adv* **5**, eaau6455.

Zhang, J., Houston, D. W., King, M. L., Payne, C., Wylie, C. and Heasman, J. (1998). The role of maternal VegT in establishing the primary germ layers in Xenopus embryos. *Cell* **94**, 515-524.

Zorn, A. M. and Wells, J. M. (2009). Vertebrate endoderm development and organ formation. *Annu Rev Cell Dev Biol* **25**, 221-251.

Figures

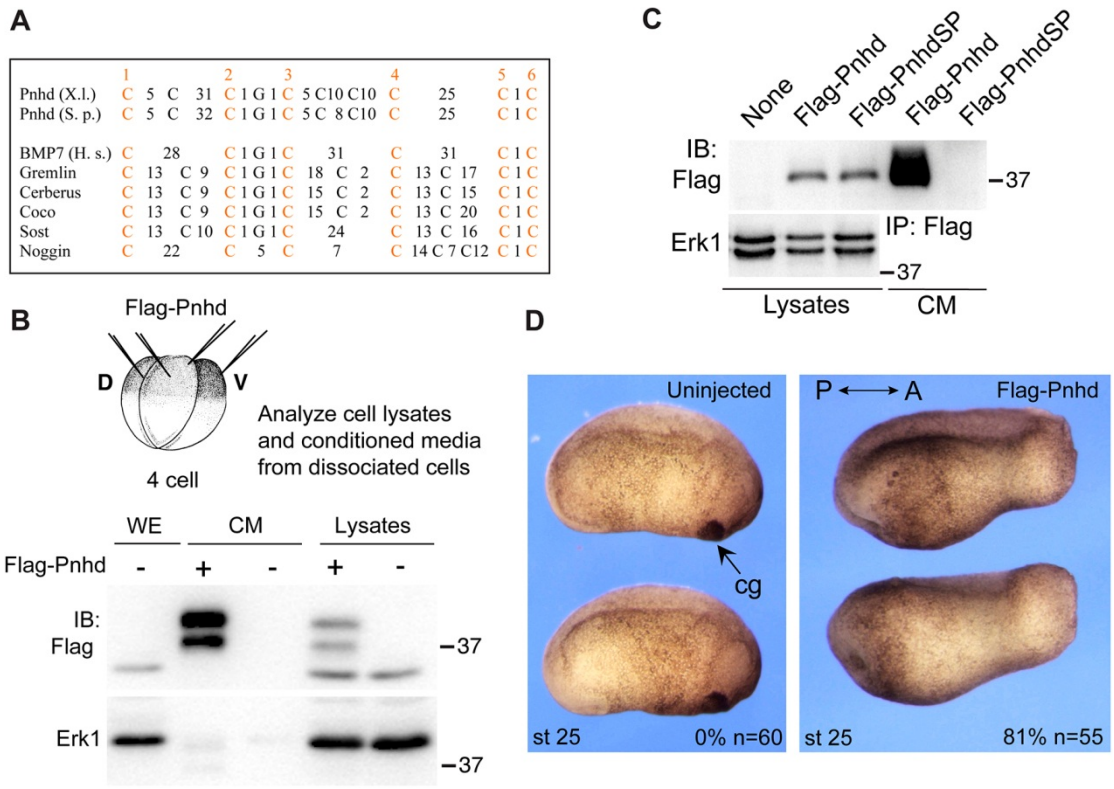

Fig. 1. Pnhd is a secreted protein that promotes posterior development.

A, Alignment of cystine-knot (CK) domains from Pnhd and other secreted proteins. Spacing is indicated by numbers of nonconserved amino acids between conserved cysteine residues. *X.l., Xenopus laevis; S.p. Stegastes partitus; H.s., Homo sapiens.* B, Secretion of Pnhd by *Xenopus* gastrula cells. Four-cell embryos were injected with 0.5 ng of Flag-Pnhd RNA per each blastomere, cultured to the onset of gastrulation and dissociated to individual cells. Pnhd levels were compared in the media conditioned for 3 hrs and the corresponding cell lysates. C, Pnhd is secreted by transfected HEK293Tcells. Deletion of the putative signal peptide in PnhdSP prevents secretion. WE, whole embryo; CM, conditioned medium (B, C). D, Head defects in embryos injected dorsally with 2 ng of *pnhd* RNA at the 4-cell stage. Frequencies of

embryos with head defects and their total number are indicated. cg, cement gland. The results are representative of more than five independent experiments.

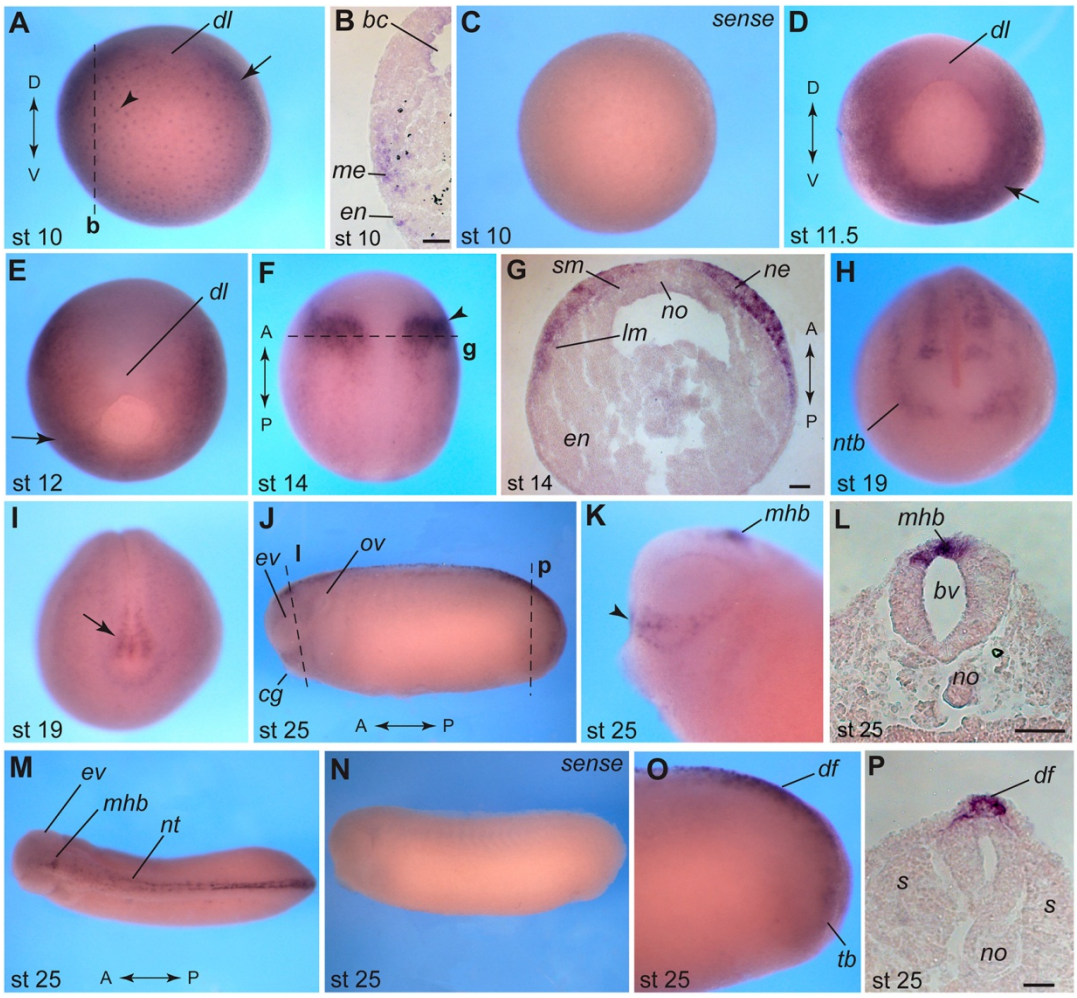

Fig. 2. Pnhd transcript localization at different developmental stages.

Wholemount *in situ* hybridization has been carried out with albino embryos using *pnhd* antisense and sense RNA probes. A, Stage 10 embryo. Vegetal view, dorsal is up. Arrowhead points to vegetal endoderm. B, Cross-section of a stage 10 embryo. C, Control embryo, stage 10 (sense probe). D, stage 11.5 embryo, vegetal view, dorsal is up. E, stage 12 embryo, vegetal view, dorsal side is up. Arrows in A, D, E point to mesodermal expression. F, Dorsal view stage 14 embryo, anterior is up. Arrowhead marks neuroectoderm. G, Cross-section of embryo shown in F. H, stage 19 embryo, anterior view, dorsal is up. I, stage 19, posterior view, dorsal is up. Arrow points to staining in the tailbud.

J, stage 25 embryo, side view. K, stage 25 embryo, head, anterior is left. Arrowhead points to the signal in the superficial ectoderm cells that are dorsal to the cement gland. J, K, M-O, anterior is to the left. L, Cross-section corresponding to the midbrain level of embryo in (J). M, stage 25, dorsal view. N, stage 25, control sense probe. O, stage 25 embryo, lateral view of tailbud. P, Transverse section corresponding to J and O. Dashed lines mark the approximate level of corresponding sections (indicated by bold letters). Dorsoventral (D/V) and anteroposterior (A/P) embryonic axes are indicated, Scale bar is 50 μm in all panels except in panel P, 25 μm. Abbreviations: dl, dorsal blastopore lip.; bc, blastocoel; bv, brain ventricle; me, mesoderm; en, endoderm; ne, neuroectoderm, sm, somitic mesoderm; lm, lateral mesoderm; no, notochord; ev, eye vesicle; ov, otic vesicle; cg, cement gland; ntb, neural tube border; nt, neural tube; mhb, midbrain-hindbrain boundary; df, dorsal fin; tb, tailbud, s, somites.

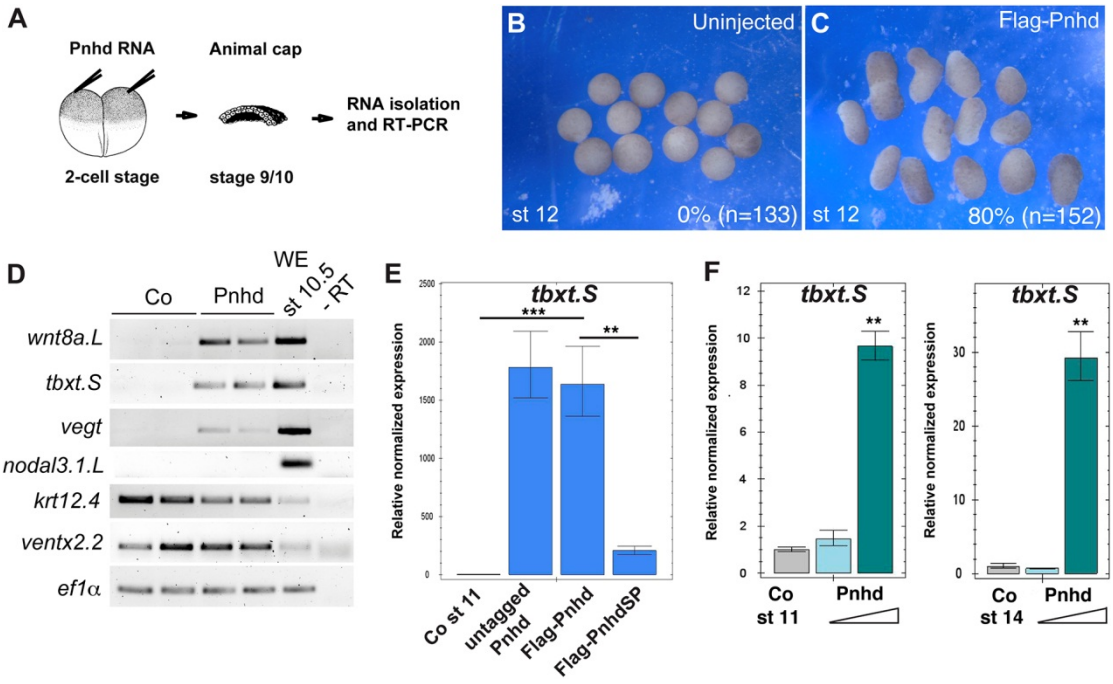

Fig. 3. Pnhd induces mesoderm in ectodermal explants. A-E, Early embryos were injected with 1-2 ng of Pnhd RNA. Ectoderm explants were dissected at late blastula stages and cultured until stage 12 to examine morphology (B, C) and gene expression by RT-PCR (D, E). B, C, Pnhd RNA induced animal cap elongation by stage 12. Frequencies of elongated explants and their total number are indicated. The results represent more than 5 independent experiments. D, Induction of selected mesodermal markers by Flag-Pnhd RNA (1 ng); E, Flag-Pnhd RNA has the same ability to induce *tbxt* as untagged Pnhd RNA in RT-qPCR, but this activity is lost in Flag-PnhdSP, lacking the signal peptide (2 ng of each RNA). F, Pnhd protein has been purified from the supernatants of transfected HEK293T cells. To assess its mesoderm-inducing activity, ectoderm explants were dissected from stage 10 embryos and cultured in 0.6 x MMR solution containing 1.5 µg/ml or 6.5 µg/ml of Pnhd. RT-qPCR was carried out for *tbxt* and cdx4 (not shown) at stage 11 or stage 14. Significance was determined by the two-tailed Student's t-test, $p<0.01$ (**) and $p<0.001$ (***).

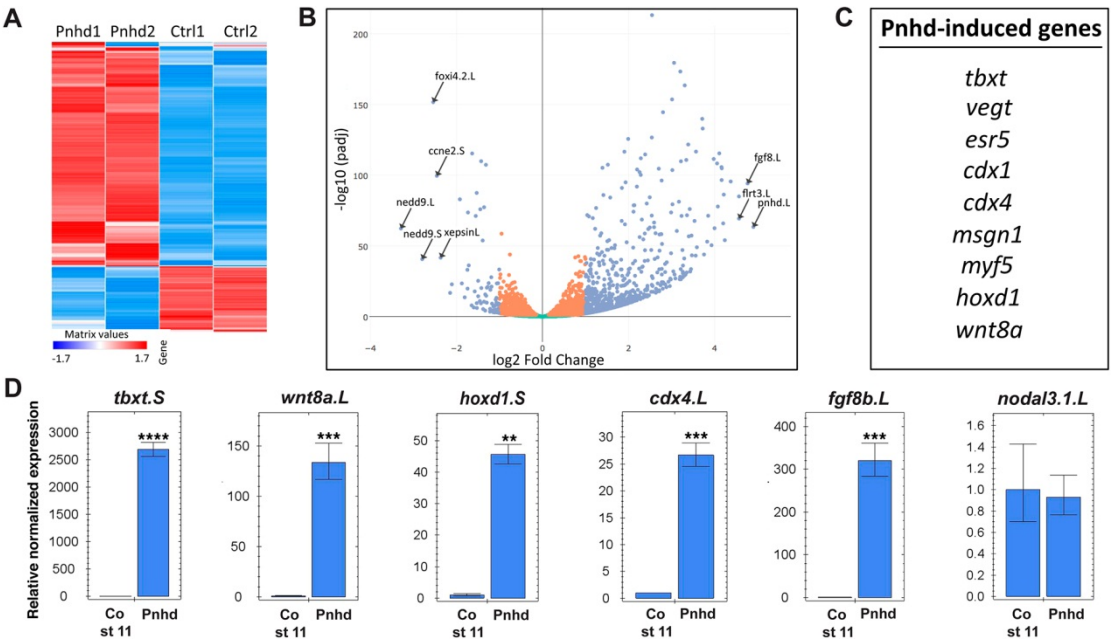

Fig. 4. RNA sequencing defines Pnhd target genes. A, Heatmap of gene expression in the Pnhd-expressing and control uninjected animal pole cells that were cultured until stage 11/12. The duplicate samples are highly similar. B, Volcano plot shows top genes upregulated by Pnhd. C, Differentially expressed genes that are induced by Pnhd RNA (1.5 ng) in animal caps. The list was derived from the top 100 genes induced by Pnhd in four independent RNAseq experiments. D, qRT-PCR validation of Pnhd targets in animal caps.

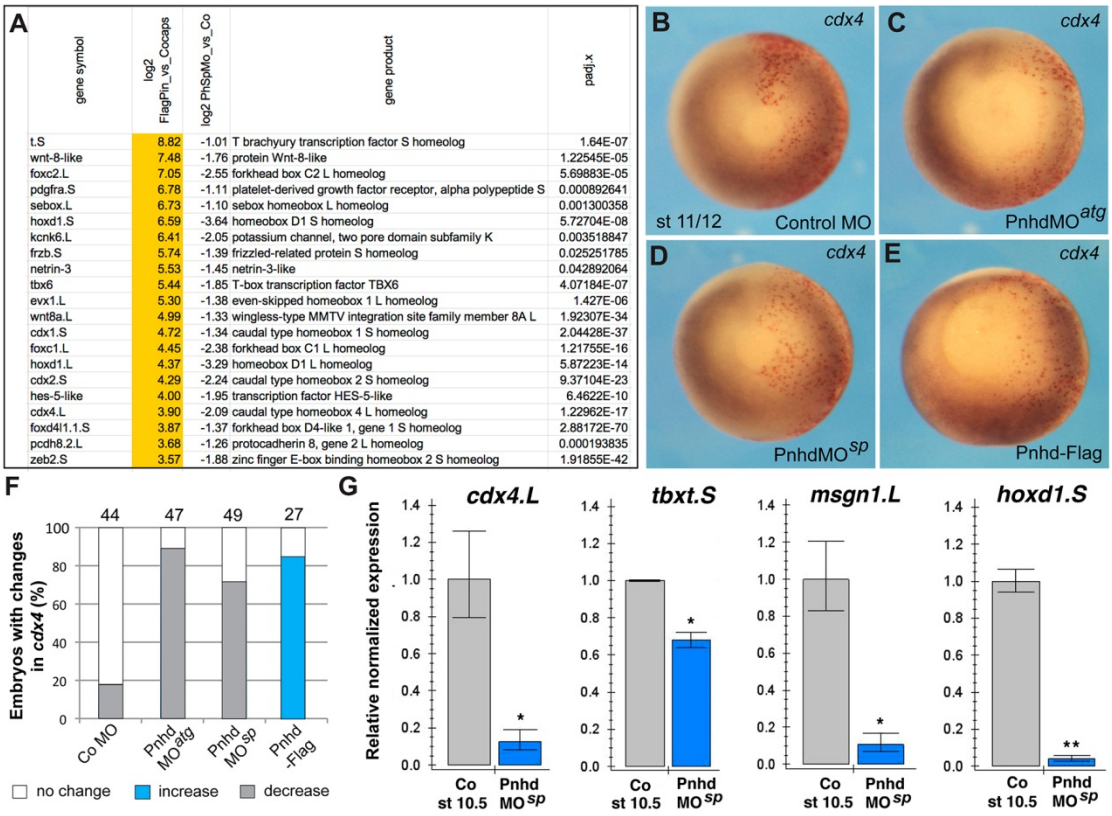

Fig. 5. Pnhd is required for mesoderm formation. A, Top differentially expressed Pnhd gene targets in the marginal zone. The list has been sorted by log2-fold induction in response to *flag-pnhd* RNA (1.5 ng) and selected for the genes downregulated by *pnhd* MO^{sp}. For pnhd knockdown, 10 ng of *pnhd* MO^{atg} or 40 ng of *pnhd* MO^{sp} were injected two to four times into marginal zone of four-cell embryos. RNA has been extracted from marginal zone explants at stage 10.5. B-E, Whole mount *in situ* hybridization validates changes in *cdx4* expression in embryos with manipulated Pnhd levels in one half of each embryo. RedGal was used as a β-galactosidase substrate (red) for lineage tracing of the injected area. Compare gene expression (dark blue) between the injected (red) and uninjected sides. F, Quantification of changes in *cdx4* RNA in Pnhd-depleted or overexpressing embryos. G, RT-qPCR confirms the downregulation of *cdx4, hoxd1, msgn1* and *tbxt* in stage 10.5

marginal zone explants depleted of *pnhd*. Means +/- standard errors are shown. Significance was determined by the two-tailed Student's t-test, $p<0.05$ (*), $p<0.01$ (**).

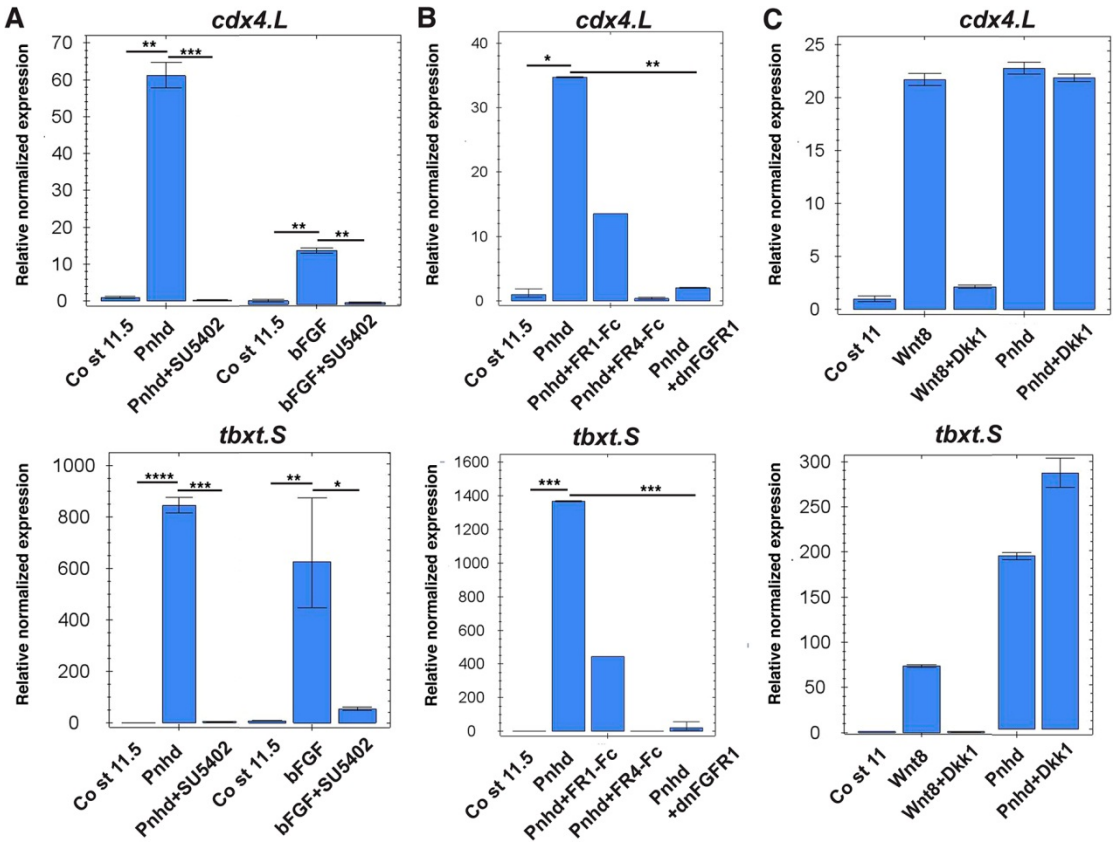

Fig. 6. Pnhd response requires FGF but not Wnt signaling. Embryos were injected in the animal pole region at the 2-cell stage with 1-2 ng of Pnhd RNA, FGFR1-Fc, FGFR4-Fc, or dnFGFR1 RNA (2 ng each), 1 ng of Wnt8 or 300 pg of Dkk1 RNA as indicated. Ectoderm explants were dissected at stages 9-10 and cultured until stage 11-11.5 for gene expression analysis by RT-qPCR. A, The induction of *tbxt* and *cdx4* by Pnhd is blocked by the FGF inhibitor SU5402 (100 µm). Stimulation with bFGF was a positive control. B, Gene target activation by Pnhd was prevented by DN-FGFR1 and secreted forms of FGFR1-Fc and FGFR4-Fc. C, The Wnt inhibitor Dkk1 did not affect Pnhd signaling but effectively blocked Wnt8 responses. Means +/- standard errors are shown. Significance was determined by the two-tailed Student's t-test, $p<0.05$ (*), $p<0.01$ (**), $p<0.001$ (***), $p<0.0001$ (****).

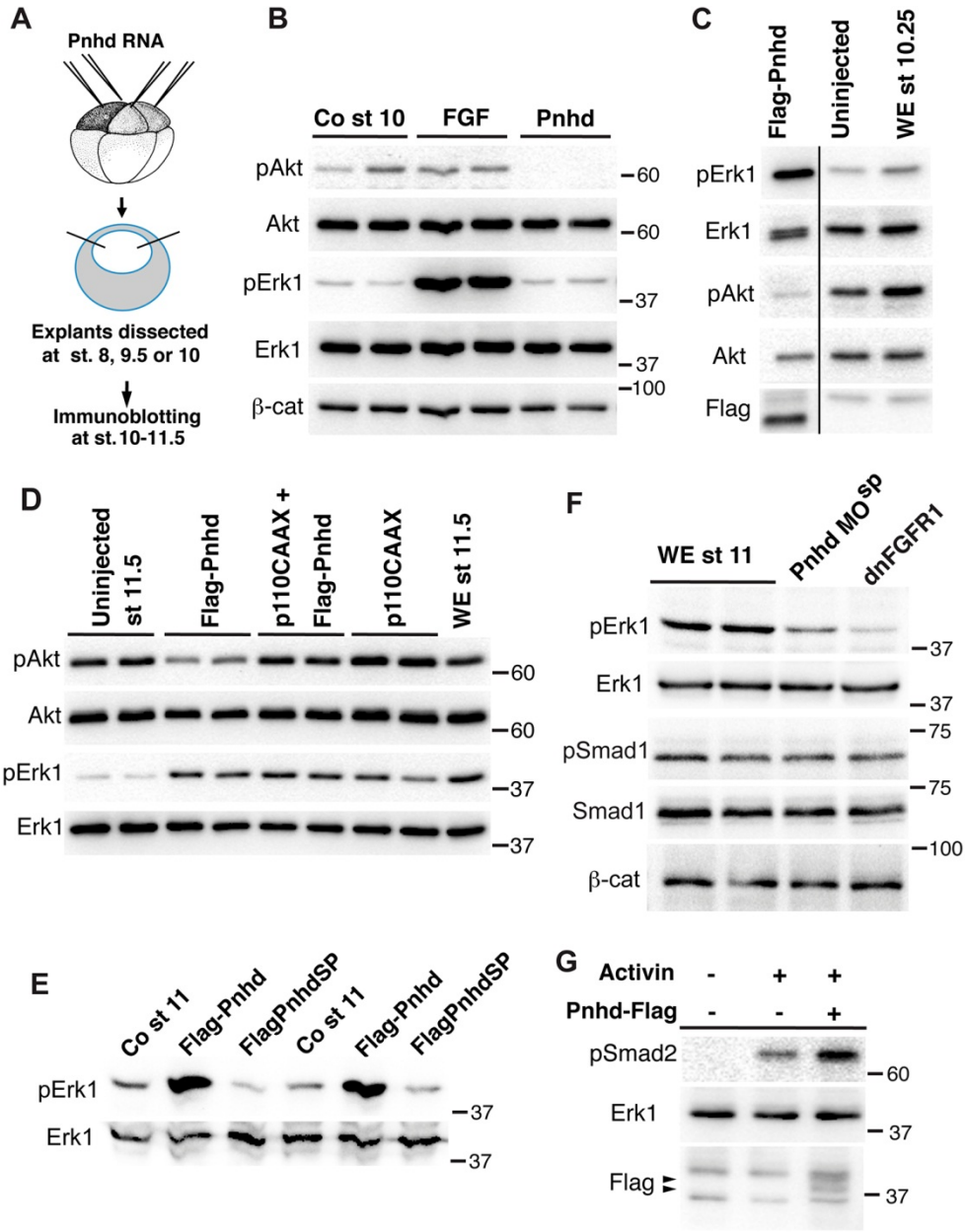

Fig. 7. Pnhd inhibits Akt, but activates Erk1. A, Scheme of the experiments shown in B-D. Embryos were injected with RNAs encoding Flag-Pnhd (1.5 ng), p110CAAX (0.5 ng), or treated with FGF protein as indicated. Ectoderm explants were dissected at stage 8, 9.5 or 10, and cultured until the desired stage for immunoblotting with indicated antibodies. B, Comparison of Pnhd and FGF effects on blastula ectoderm. Pnhd inhibits Akt phosphorylation in ectoderm explants isolated at stage 8 and analyzed at

stage 10. FGF has no effect on Akt, but activates Erk. C. Pnhd inhibits Akt, but induces Erk phosphorylation in ectoderm isolated at stage 9.5 and cultured until stage 10.25. This result has been obtained in at least 10 experiments. WE, whole embryo controls in C, D, and F. D, Pnhd-dependent stimulation of Erk is not affected by the Akt activator p110CAAX. E, Erk1 phosphorylation in Pnhd-expressing embryos at stage 11. Embryos were injected with RNAs encoding Flag-Pnhd or Flag-PnhdSP (1.5 ng each). F, Downregulation of Erk1 phosphorylation in lysates of stage 11 embryos injected with Pnhd MO^{sp}. Embryos were injected with RNAs encoding dnFGFR1 (1.5 ng each) or 40 ng of Pnhd MO^{sp} as indicated. There are no detectable changes in β-catenin or phospho-Smad1. G. Pnhd promotes Smad2 phosphorylation by Activin. Ectoderm explants were dissected from the injected embryos at stage 8 and cultured for 1 hr with or without Activin. Immunoblot analysis with anti-pSmad2 antibodies is shown. Pnhd is detected by anti-Flag antibodies (arrowhead). Erk1 is a control for loading.

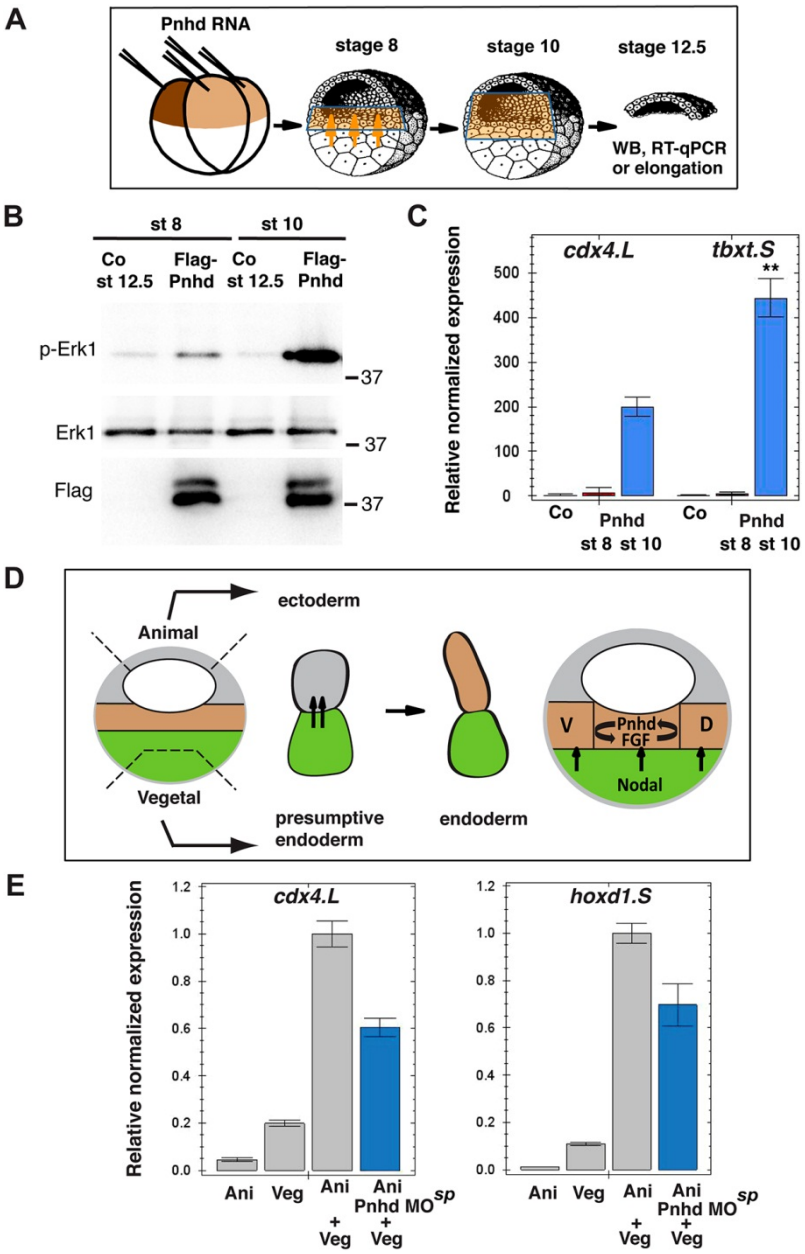

Fig. 8. Pnhd cooperates with endogenous inducing signals to promote mesoderm formation during gastrulation. A, Scheme of the experiments presented in B, C. Mesoderm-inducing signals are indicated by orange arrows. Each animal blastomere of 2-cell embryos received 1 ng of Pnhd RNA. Pnhd-expressing or control ectoderm explants were isolated at stage 8 or stage 10, as indicated. When the control embryos reached stage 12.5, the explants were lysed for immunoblotting with antibodies specific for pErk1 and

Erk (B) and for RT-qPCR analysis of *cdx4* and *tbxt* transcripts (C). B, Erk is synergistically activated by Pnhd and endogenous signals in ectoderm explants isolated at stage 10. C, cooperative activation of mesodermal gene targets by Pnhd and endogenous signals in ectoderm dissected at stage 10. D, E. Pnhd is required for mesoderm formation in response to endogenous inducing signals. D, Scheme of the experiment shown in E. Model for Pnhd function (right panel). Pnhd is activated in the marginal zone by Nodal and FGF signaling and functions within the newly induced mesodermal layer. V- ventral mesoderm, D, dorsal mesoderm. E, Pnhd is required for mesoderm formation in animal-vegetal conjugates. Pnhd MO^{sp}-injected or control animal pole explants were combined with vegetal explants at stage 8. After the culture until stage 11, levels of *cdx4* and *hoxd1* transcripts were determined in the conjugates by RT-qPCR.

Fig. S1

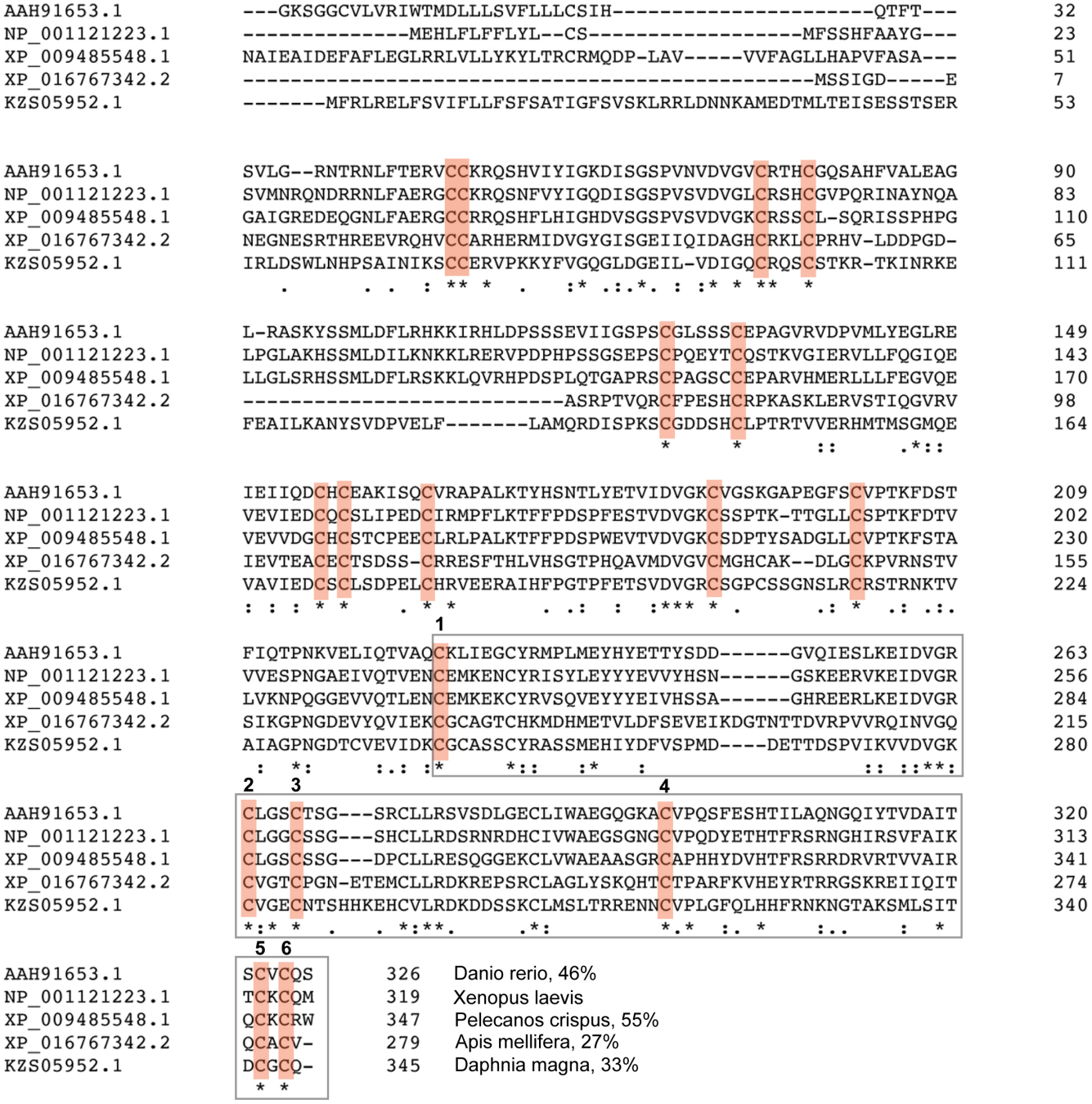

Figure S1. Alignment of Pnhd homologs. Multiple protein sequences that are similar to Pnhd from different species have been aligned using ClustalOmega from EBI. Percent identity to *Xenopus laevis* Pnhd.L protein is shown for Pnhd homologs from *Danio rerio, Pelecanus crispus, Apis mellifera, and Daphnia magna*. All three cystine knot domains marked by characteristic Cys residues appear conserved in different Pnhd proteins (asterisks).

Fig. S2

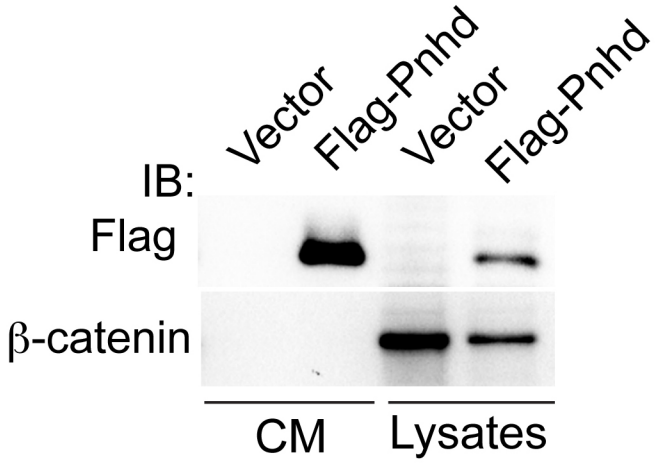

Figure S2. Pnhd secretion in cultured cells. A, HEK293T cells were transfected with *Pnhd-Flag-pCS2* DNA or control *pCS2* DNA and cultured for 48 hrs. Proteins from cell lysates or corresponding conditioned media were separated by SDS-PAGE and immunoblotted with anti-Flag antibodies. β-catenin is a control for protein loading.

Fig. S3

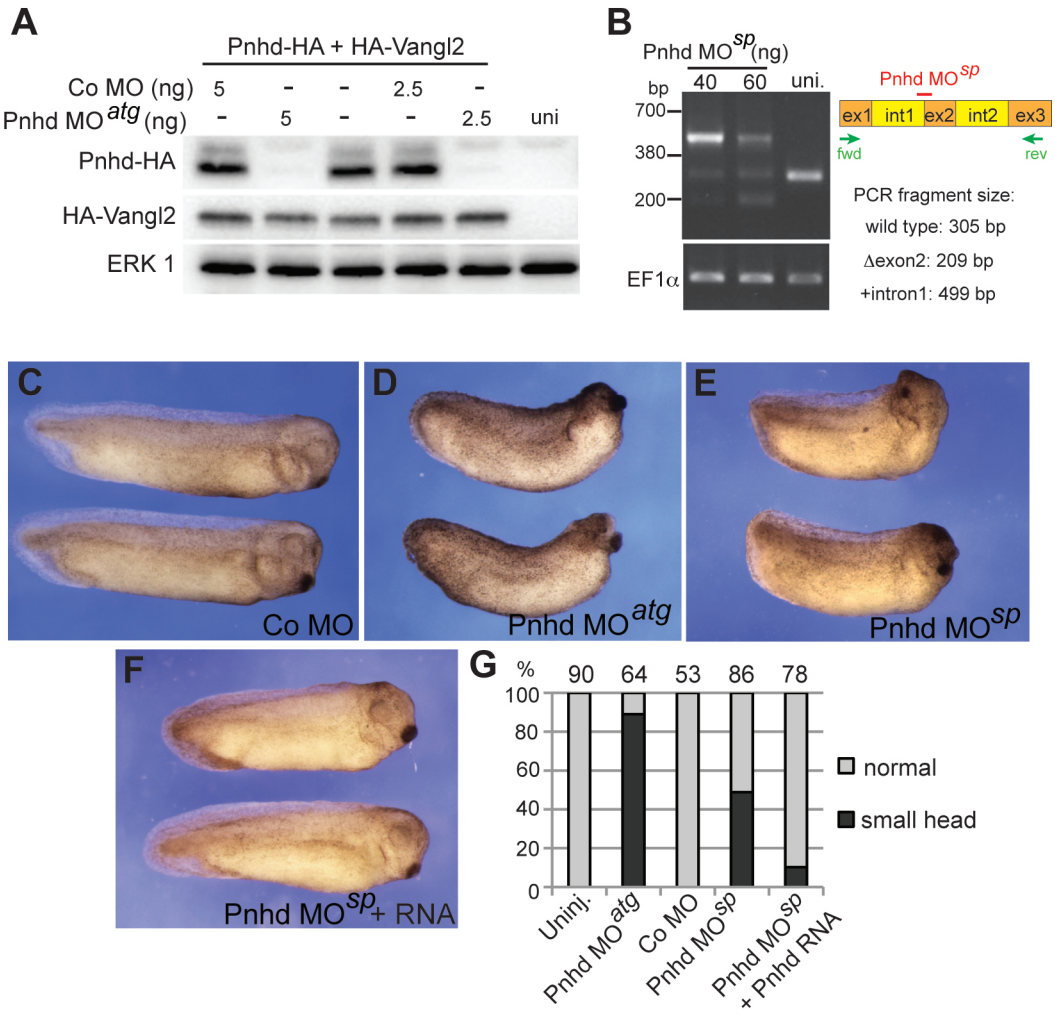

Figure S3. Validation of *pnhd* knockdown. A, Translation-blocking MO inhibits *pnhd-HA* RNA translation *in vivo*. Embryos were coinjected with *pnhd-HA*-RNA and *HA-vangl2* RNA (negative control) in the presence of a control (Co) or *pnhd* MO^{atg} (10 ng each) as indicated. Immunoblotting with anti-HA antibodies shows specific inhibitory effect of *pnhd* MO^{atg} on Pnhd protein levels. B, *pnhd* MO^{sp} (40-60 ng) interferes with endogenous Pnhd RNA splicing in morphants. C-F, Morphological phenotypes of embryos depleted of Pnhd (C-E). F, *pnhd* RNA (10 pg) rescues the morphant phenotype (F). G. Quantification of data presented in (C-F).

Fig. S4

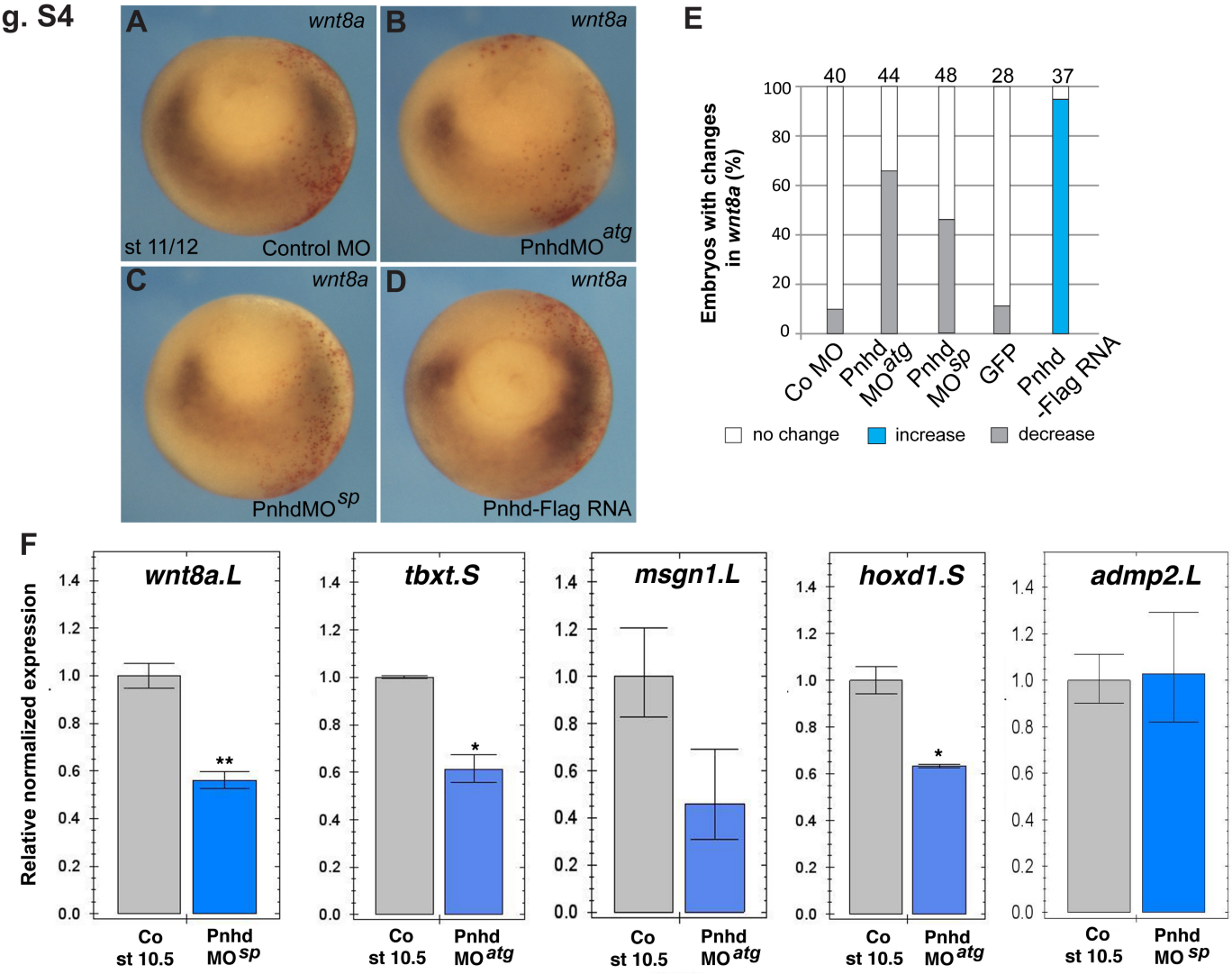

Figure S4. Regulation of *wnt8a* transcription by Pnhd. A-D, Whole mount in situ hybridization validates changes in *wnt8a* expression in embryos with manipulated *pnhd*. Injection experiments were performed as described in Fig. 5B-F. Wnt8 transcripts are visible as dark blue staining. RedGal is a lineage tracer. Representative embryos are shown. E, quantification of the results shown in A-D. F, RT-qPCR confirms downregulation of *wnt8a.L, tbxt.s*, *msgn1.L* and *hoxd1.s* in stage 10.5 marginal zone explants depleted of Pnhd. By contrast, the ventral marker *admp2* is not affected by Pnhd depletion.

Fig. S5

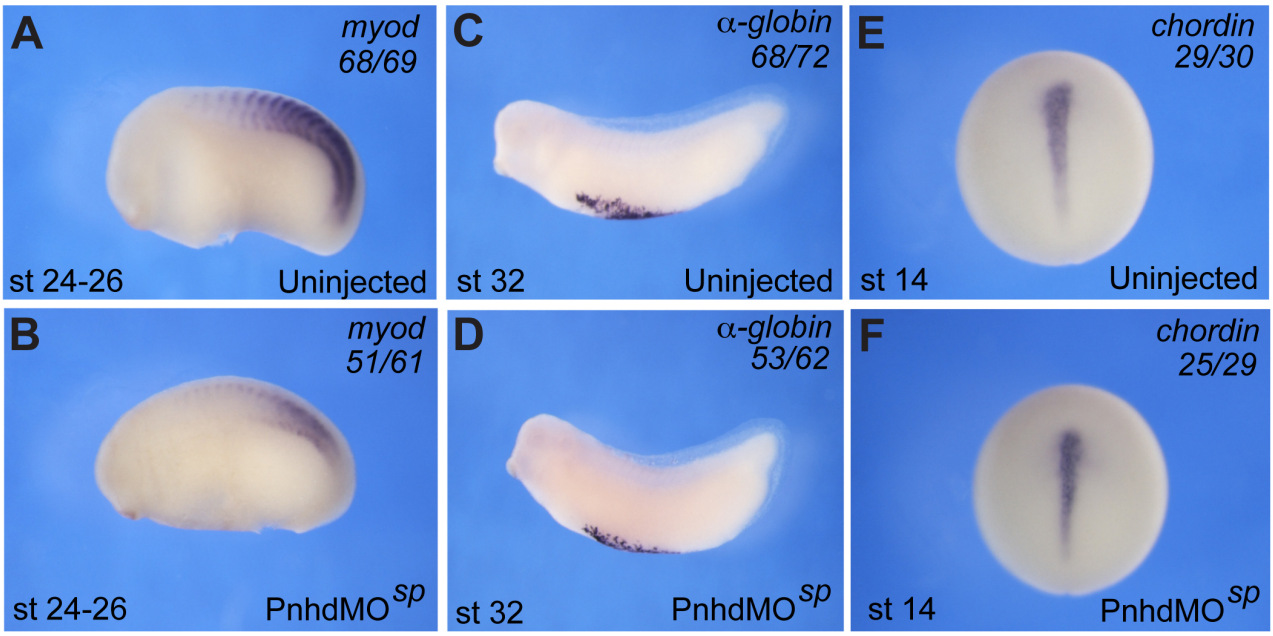

Figure S5. Regulation of mesodermal gene expression by Pnhd .

For *pnhd* depletion, each blastomere of four-cell embryos has been injected with 40 ng of *pnhd* MO^{sp}. The uninjected controls (A, C, E) or *pnhd* morphants (B, D, F) have been cultured until the indicated stages, fixed and processed for wholemount *in situ* hybridization with anti-sense probes that are specific for *myod* (A, B), *α-globin* (C, D) and *chordin* (E, F). Number of embryos with the presented phenotype (top) and the total number of embryos per group (bottom) are shown.

Fig. S6

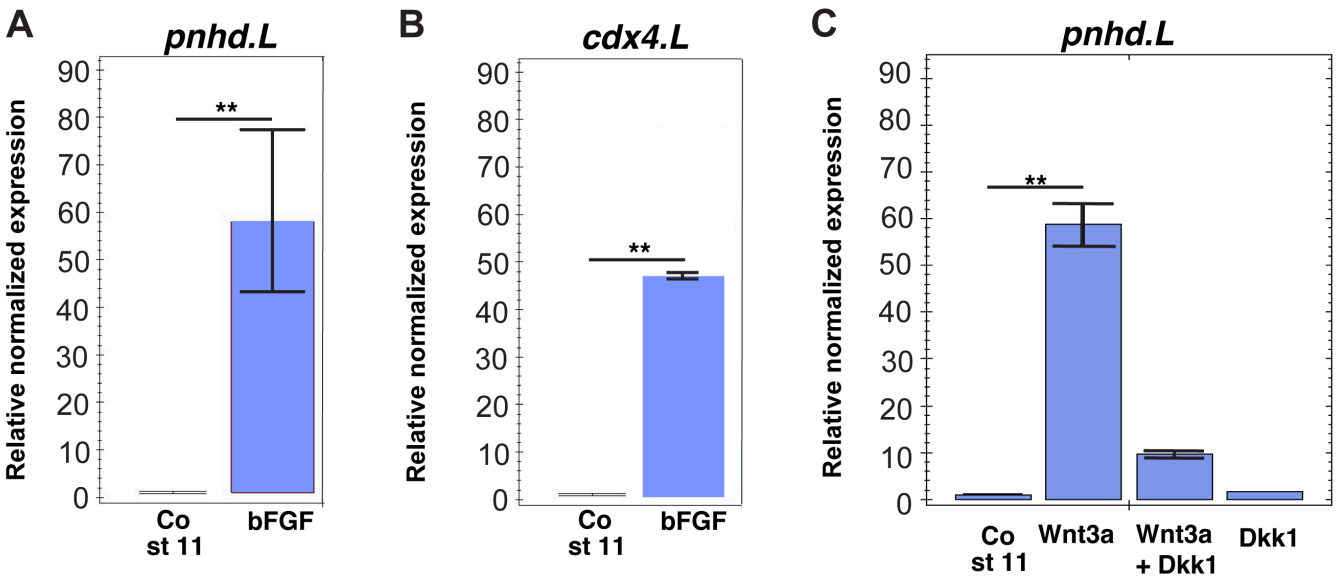

Figure S6. Pnhd transcripts are induced in ectoderm by FGF and Wnt signals. RT-qPCR data from animal caps treated with FGF or expressing Wnt3a. Ectoderm explants were dissected at stage 9-10 and cultured until stage 11. A, B, The induction of *pnhd* and *cdx4* by FGF. C, *Pnhd* transcription is activated by Wnt3a and this effect is blocked by Dkk1. Means +/- standard errors are shown. Significance was determined by the two-tailed Student's t-test, $p<0.01$ (**).

Fig. S7

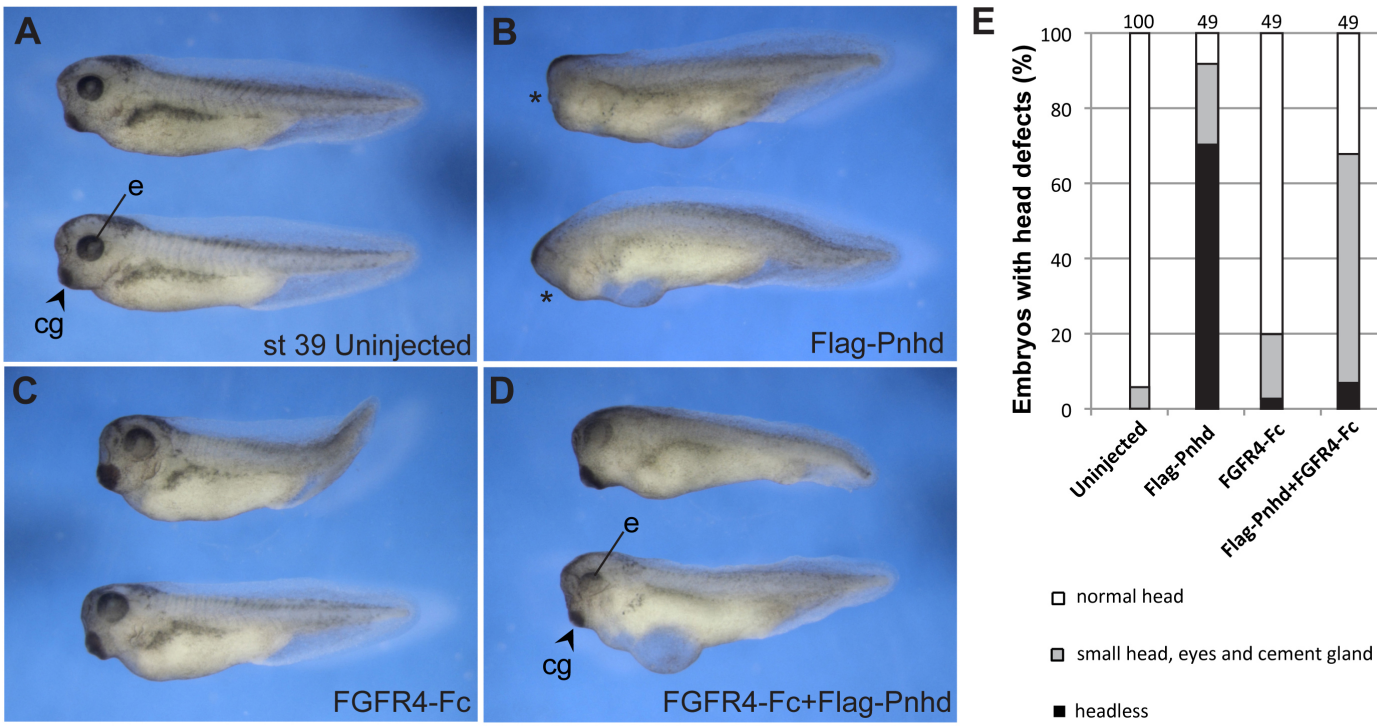

Figure S7. Secreted dominant-interfering form of FGFR4 rescues head deficiency caused by Pnhd. Four-cell embryos have been injected with indicated RNAs, morphological phenotypes were scored at stage 39. A, Uninjected control embryos. B. Lack of head structures (*) in embryos injected with *pnhd* RNA (0.9 ng). C. Mild posterior defects in embryos injected with *FGFR4-Fc* RNA (20 pg). D. Coinjection of *FGFR4-Fc* RNA rescued the headless phenotype. Arrows and arrowheads in A and D point to eyes (e) and cement glands (CG), respectively. E. Quantification of the results. The data are representative of two different experiments.

Fig. S8

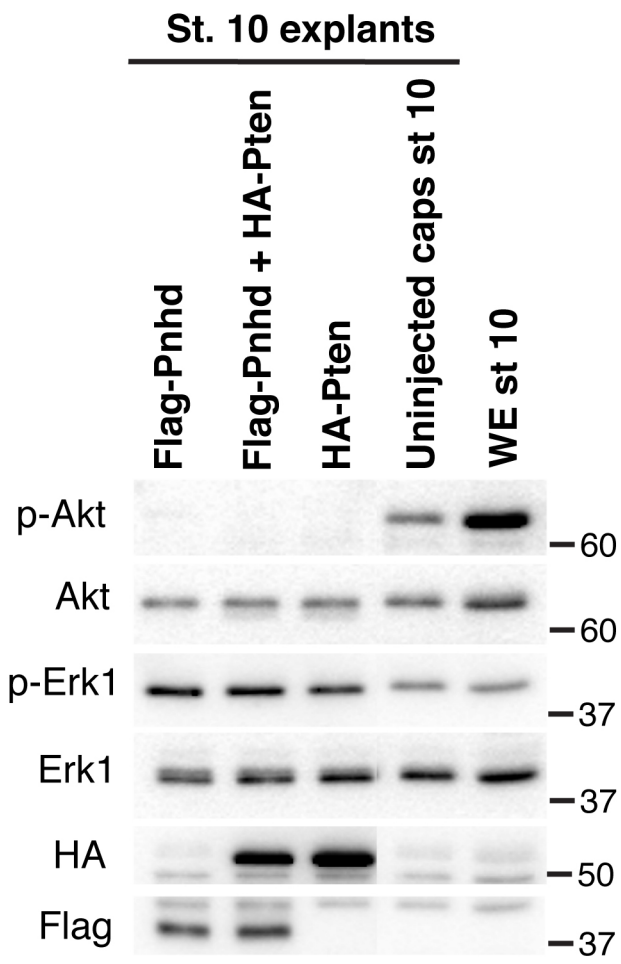

Figure S8. Akt inhibition by Pten does not influence Pnhd signaling.

Embryos were injected with RNAs encoding Flag-Pnhd (1.5 ng) or Pten (0.5 ng), as indicated. Ectoderm explants were dissected at stage 9.5, and cultured until stage 10.25 for immunoblotting with indicated antibodies. Pnhd inhibits Akt, but induces Erk phosphorylation in ectoderm at late blastula stages. When coinjected with Pnhd, Pten further inhibits Akt but does not alter Pnhd-dependent Erk activation.

Fig. S9

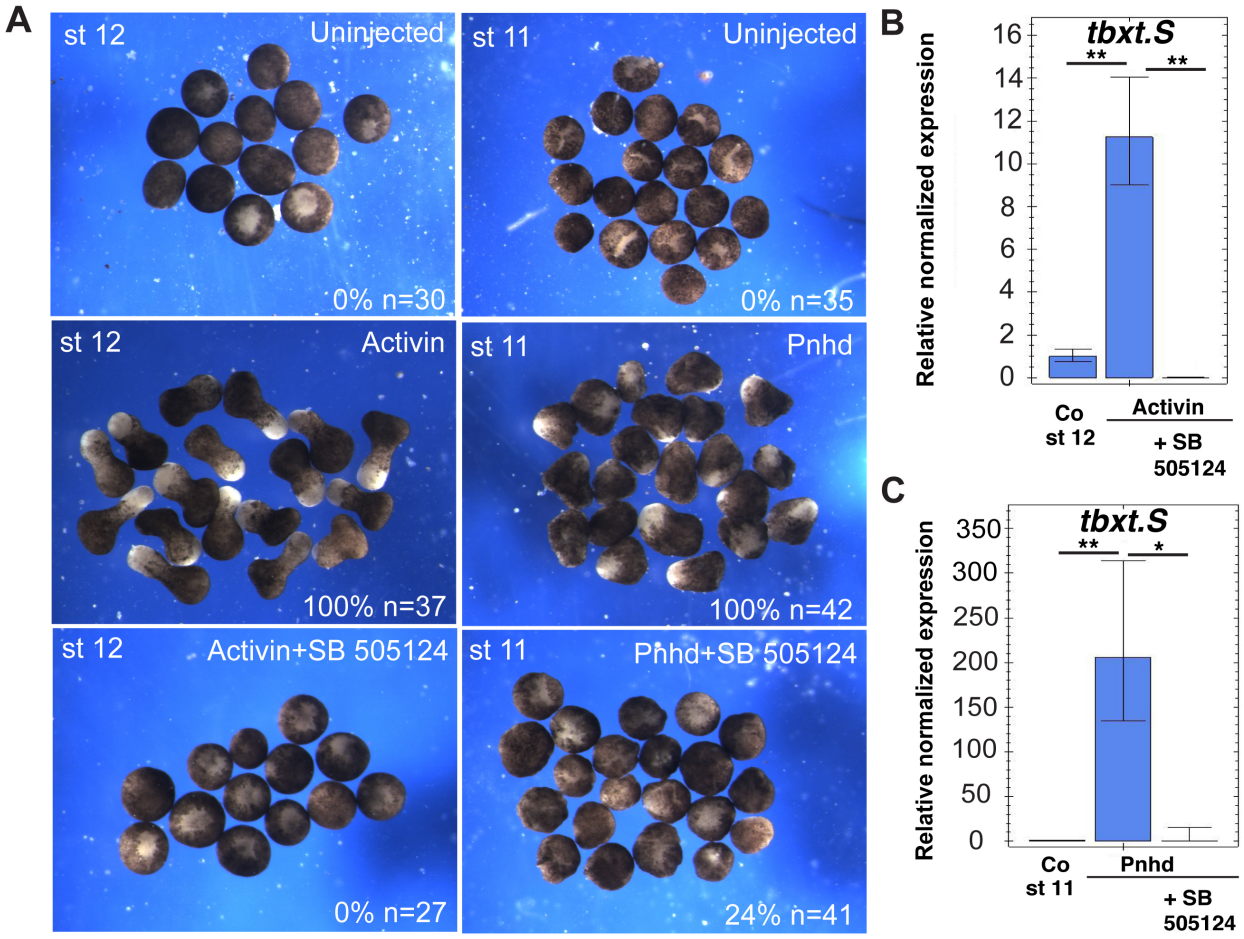

Figure S9. Pnhd activity is blocked by the Nodal/Activin inhibitor SB505124.

Animal caps were dissected at stage 9-10 and stimulated with Activin or obtained from embryos injected with pnhd RNA. RT-qPCR analysis of *tbxt.S* transcripts was carried out in animal caps incubated in the presence or absence of SB505124. A, Effect of SB505124 on Activin- or Pnhd-dependent mesoderm induction. Frequencies of the shown morphological changes and the total number of explants per group are indicated. Data are representative of three independent experiments. B, RT-qPCR analysis of *tbxt.S* transcripts in animal caps treated with Activin in the presence or absence of SB505124. C, Pnhd-dependent induction of *tbxt.S* in the presence or absence of SB505124. Means +/- standard errors are shown. Significance was determined by the two-tailed Student's t-test, $p<0.01$ (**).

Fig. S10

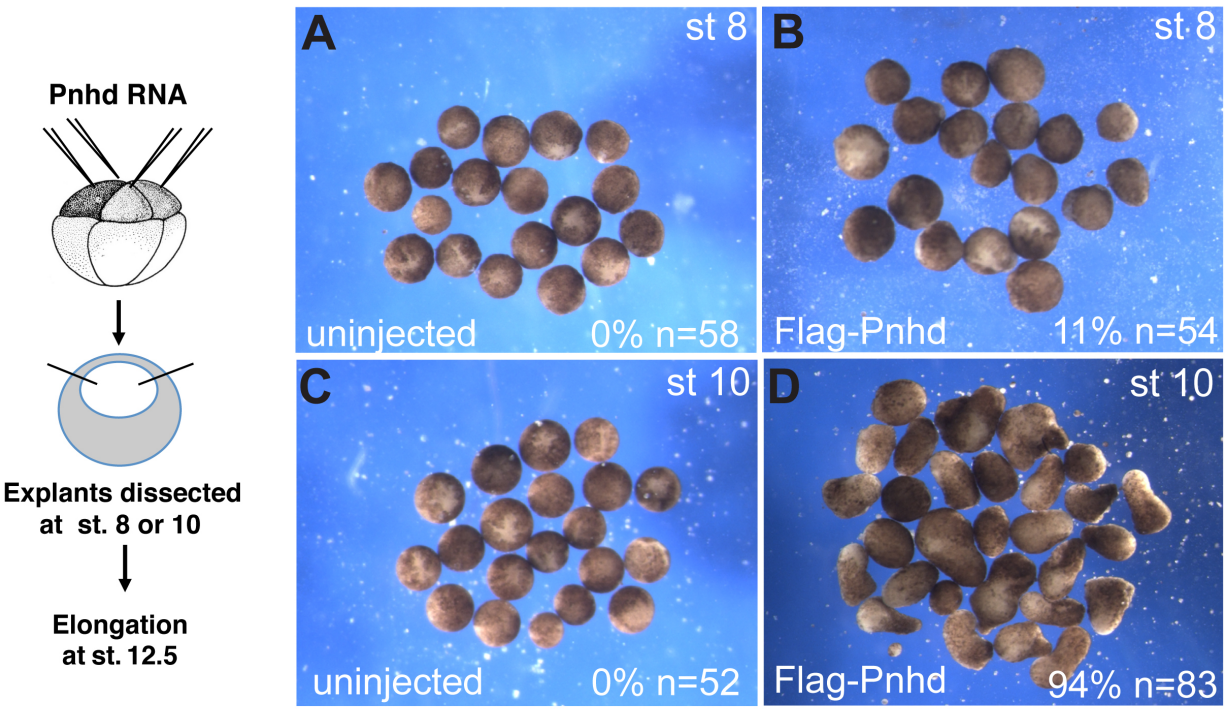

Figure S10. Pnhd-dependent elongation of animal caps isolated at the onset of gastrulation. Animal cap explants were prepared at stage 8 (A, B) or stage 10 (C, D) from the control uninjected (A, C) or *pnhd* RNA (2 ng)-injected (B, D) embryos and were cultured until stage 12.5, at which point explant morphology was imaged. Frequencies of explant elongation and total numbers of explants per group are shown. Data are representative of three independent experiments.

Fig. S11

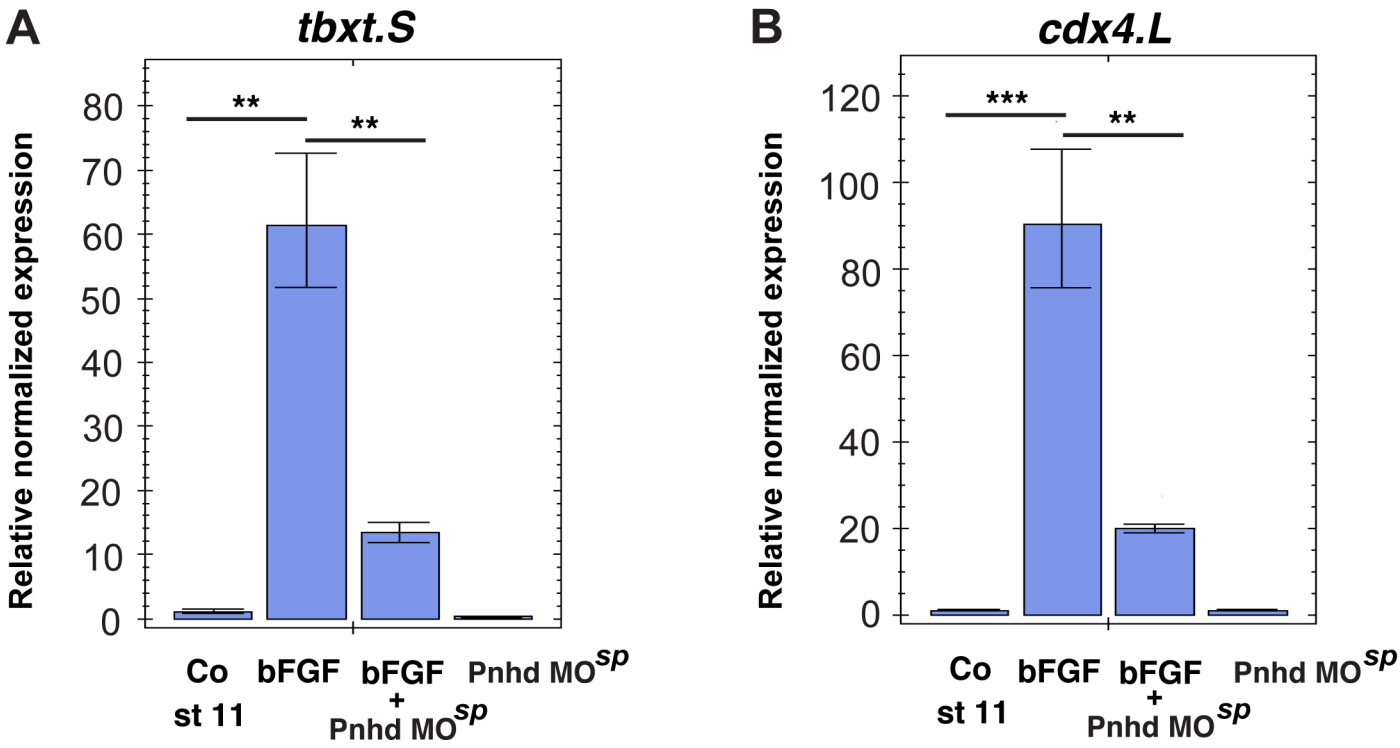

Figure S11. Pnhd is required for FGF-dependent mesoderm induction.

A, B, RT-qPCR was carried out for *cdx4* and *tbxt* in ectoderm lysates from Pnhd-depleted or control embryos after FGF stimulation as indicated. Embryos were injected into each of four animal blastomeres with Pnhd MO^{sp} (30 ng) at the 8-cell stage. Ectoderm explants were dissected at stage 8-8.5 and cultured until stage 11. Means +/- standard errors are shown.

Table S1. Differentially expressed genes in ectoderm explants with ectopic *pnhd* RNA.

Click here to Download Table S1

Table S2. Putative *pnhd* target genes. The list of common genes upregulated by *pnhd* RNA in ectoderm explants and reduced in the marginal zones of embryos injected with *pnhd* MO^{sp}.

Table 2. Genes that are upregulated by Pinhead overexpression and reduced by Pinhead depletion with splicing-blocking MO

	GeneNames	log2 FlagPin_vs_Cocaps	log2 PhSpMo_vs_Co	Variation in the expected sense	product (DAVID).x
		Total correct:		71	
182	t.S	8.82	-1.01	YES	T brachyury transcription factor S homeolog(t.S)
100	LOC108713288	7.48	-1.76	YES	protein Wnt-8-like(LOC108713288)
191	zg16.S	7.44	4.77		zymogen granule protein 16 S homeolog(zg16.S)
75	LOC108698139	7.10	3.04		lipocalin-like(LOC108698139)
42	foxc2.L	7.05	-2.55	YES	forkhead box C2 L homeolog(foxc2.L)
144	pdgfra.S	6.78	-1.11	YES	platelet-derived growth factor receptor, alpha polypeptide S homeolog (pdgfra.S)
163	sebox.L	6.73	-1.10	YES	sebox homeobox L homeolog(sebox.L)
58	hoxd1.S	6.59	-3.64	YES	homeobox D1 S homeolog(hoxd1.S)
60	kcnk6.L	6.41	-2.05	YES	potassium channel, two pore domain subfamily K, member 6 L homeolog (kcnk6.L)
24	col17a1.L	6.41	3.40		collagen, type XVII, alpha 1 L homeolog(col17a1.L)
78	LOC108699267	6.33	2.35		neuropeptide Y receptor type 2-like(LOC108699267)
104	LOC108714881	6.29	4.43		neural retina-specific leucine zipper protein-like(LOC108714881)
106	LOC108715253	6.10	3.35		catalase-like(LOC108715253)
47	frzb.S	5.74	-1.39	YES	frizzled-related protein S homeolog(frzb.S)
81	LOC108699331	5.66	4.52		C-reactive protein-like(LOC108699331)
88	LOC108703174	5.53	-1.45	YES	netrin-3-like(LOC108703174)
89	LOC108703928	5.44	-1.85	YES	T-box transcription factor TBX6(LOC108703928)
97	LOC108709615	5.38	3.36		multidrug and toxin extrusion protein 2-like(LOC108709615)
30	evx1.L	5.30	-1.38	YES	even-skipped homeobox 1 L homeolog(evx1.L)
98	LOC108709870	5.27	2.05		arf-GAP with GTPase, ANK repeat and PH domain-containing protein 2-like(LOC108709870)
188	wnt8a.L	4.99	-1.33	YES	wingless-type MMTV integration site family member 8A L homeolog(wnt8a.L)
80	LOC108699330	4.82	3.81		C-reactive protein-like(LOC108699330)
113	LOC108719482	4.80	3.11		neurogenic locus notch homolog protein 1-like(LOC108719482)
17	cdx1.S	4.72	-1.34	YES	caud+F28al type homeobox 1 S homeolog(cdx1.S)
109	LOC108716948	4.68	3.59		uncharacterized LOC108716948(LOC108716948)
169	slc26a9.S	4.66	3.69		solute carrier family 26 (anion exchanger), member 9 S homeolog(slc26a9.S)
134	nppb.S	4.62	3.87		natriuretic peptide B S homeolog(nppb.S)
156	rasl11b.L	4.55	1.05		RAS-like family 11 member B L homeolog(rasl11b.L)
93	LOC108705387	4.54	1.68		chemokine-like receptor 1(LOC108705387)
94	LOC108705532	4.52	2.42		uncharacterized LOC108705532(LOC108705532)
110	LOC108718036	4.47	2.42		multidrug resistance-associated protein 5-like(LOC108718036)
40	foxc1.L	4.45	-2.38	YES	forkhead box C1 L homeolog(foxc1.L)
57	hoxd1.L	4.37	-3.29	YES	homeobox D1 L homeolog(hoxd1.L)
19	cdx2.S	4.29	-2.24	YES	caudal type homeobox 2 S homeolog(cdx2.S)
69	LOC108696533	4.14	2.99		uncharacterized LOC108696533(LOC108696533)
137	nt5c3a.L	4.10	3.42		5'-nucleotidase, cytosolic IIIA(nt5c3a.L)
55	hars.L	4.02	2.02		histidyl-tRNA synthetase L homeolog(hars.L)
65	LOC100486127.S	4.02	1.88		cytochrome P450 2J6-like S homeolog(LOC100486127.S)
73	LOC108697694	4.00	-1.95	YES	transcription factor HES-5-like(LOC108697694)
36	fkbp9.S	3.98	1.85		FK506 binding protein 9 S homeolog(fkbp9.S)
67	LOC108696466	3.97	2.37		Down syndrome cell adhesion molecule-like protein 1 homolog(LOC108696466)
71	LOC108696801	3.96	3.59		urokinase plasminogen activator surface receptor-like(LOC108696801)
52	gjc2.L	3.92	2.86		gap junction protein gamma 2 L homeolog(gjc2.L)
20	cdx4.L	3.90	-2.09	YES	caudal type homeobox 4 L homeolog(cdx4.L)
83	LOC108700049	3.89	2.61		uncharacterized LOC108700049(LOC108700049)
43	foxd4l1.1.S	3.87	-1.37	YES	forkhead box D4-like 1, gene 1 S homeolog(foxd4l1.1.S)
107	LOC108715768	3.86	1.47		uncharacterized LOC108715768(LOC108715768)
119	mab21l2.S	3.78	1.66		mab-21-like 2 S homeolog(mab21l2.S)
142	pcdh8.2.L	3.68	-1.26	YES	protocadherin 8, gene 2 L homeolog(pcdh8.2.L)
170	socs4.S	3.65	3.16		suppressor of cytokine signaling 4 S homeolog(socs4.S)
130	mmp14.L	3.65	1.21		matrix metallopeptidase 14 L homeolog(mmp14.L)
103	LOC108714877	3.58	3.59		uncharacterized LOC108714877(LOC108714877)
190	zeb2.S	3.57	-1.88	YES	zinc finger E-box binding homeobox 2 S homeolog(zeb2.S)
62	lancl3.S	3.57	2.58		LanC like 3 S homeolog(lancl3.S)
141	parp3.L	3.55	2.81		poly(ADP-ribose) polymerase family member 3 L homeolog(parp3.L)
95	LOC108706889	3.51	-1.25	YES	uncharacterized LOC108706889(LOC108706889)
13	ccdc141.S	3.50	2.96		coiled-coil domain containing 141 S homeolog(ccdc141.S)
68	LOC108696532	3.49	3.37		uncharacterized LOC108696532(LOC108696532)
70	LOC108696558	3.47	2.03		ankyrin repeat domain-containing protein 65-like(LOC108696558)
39	foxb1.L	3.46	-2.02	YES	forkhead box B1 L homeolog(foxb1.L)
176	tmprss9.S	3.45	-1.59	YES	transmembrane protease, serine 9 S homeolog(tmprss9.S)
157	rbl2.L	3.44	3.04		retinoblastoma-like 2 L homeolog(rbl2.L)
21	cdx4.S	3.38	-2.18	YES	caudal type homeobox 4 S homeolog(cdx4.S)
10	c9.L	3.35	2.81		complement component 9 L homeolog(c9.L)
9	c3ar1.L	3.31	3.84		complement component 3a receptor 1 L homeolog(c3ar1.L)
7	aplnr.S	3.25	2.53		apelin receptor S homeolog(aplnr.S)
22	chst2.S	3.24	1.19		carbohydrate (N-acetylglucosamine-6-O) sulfotransferase 2 S homeolog(chst2.S)
136	nrp2.S	3.20	-1.52	YES	neuropilin 2 S homeolog(nrp2.S)
143	pdgfra.L	3.18	-1.14	YES	platelet-derived growth factor receptor, alpha polypeptide L homeolog(pdgfra.L)
26	ednra.S	3.17	-2.24	YES	endothelin receptor type A S homeolog(ednra.S)
6	aplnr.L	3.12	1.12		apelin receptor L homeolog(aplnr.L)
118	mab21l2.L	3.09	1.22		mab-21-like 2 L homeolog(mab21l2.L)
153	ptpn14.S	3.08	2.11		protein tyrosine phosphatase, non-receptor type 14 S homeolog(ptpn14.S)
18	cdx2.L	3.06	-2.16	YES	caudal type homeobox 2 L homeolog(cdx2.L)
128	MGC80829	3.05	1.53		MGC80829 protein(MGC80829)
3	adora2a.S	3.04	1.97		adenosine A2a receptor S homeolog(adora2a.S)
161	ror2.S	3.04	-1.09	YES	receptor tyrosine kinase-like orphan receptor 2 S homeolog(ror2.S)
177	tnfrsf6b.L	3.03	4.33		tumor necrosis factor receptor superfamily member 6b L homeolog(tnfrsf6b.L)
160	rnf24.L	2.99	2.06		ring finger protein 24 L homeolog(rnf24.L)
102	LOC108714552	2.95	1.27		urotensin-2 receptor-like(LOC108714552)
14	ccng1.L	2.92	2.11		cyclin G1 L homeolog(ccng1.L)
114	LOC398134	2.91	-1.24	YES	p75-like transmembrane protein fullback(LOC398134)
152	prickle1.S	2.90	1.04		prickle homolog 1 S homeolog(prickle1.S)
91	LOC108704851	2.81	1.99		uncharacterized LOC108704851(LOC108704851)
37	fosl1.L	2.78	-3.23	YES	FOS-like antigen 1 L homeolog(fosl1.L)
2	admp2.L	2.76	-1.94	YES	antidorsalizing morphogenetic protein 2 L homeolog(admp2.L)
145	pidd1.L	2.74	1.61		p53-induced death domain protein 1 L homeolog(pidd1.L)
86	LOC108700532	2.70	1.48		methionine--tRNA ligase, mitochondrial-like(LOC108700532)
165	sesn1.L	2.70	1.99		sestrin 1 L homeolog(sesn1.L)
132	ngfr.L	2.69	-1.18	YES	nerve growth factor receptor L homeolog(ngfr.L)
133	nif.L	2.69	2.14		low molecular weight neuronal intermediate filament L homeolog(nif.L)
150	plk2.S	2.68	3.27		polo-like kinase 2 S homeolog(plk2.S)
1	adap1.L	2.67	1.06		ArfGAP with dual PH domains 1 L homeolog(adap1.L)

Table S3. List of primers used for RT-PCR and RT-qPCR.

Table 3

Primers used for RT-PCR

Gene name	Forward primer	Reverse primer
wnt8a.L	5’-atg agg tcg ggt aac agt gc-3’	5’-caa agc ctc ttg cag ctt ct-3’
xbra.S	5’-gct gga agt atg tga atg gag-3’	5’-tta agt gct gta atc tct tca-3’
nodal3.1.L	5’-ctt ctg cac tag att ctg-3’,	5’-cag ctt ctg gcc aag act-3’
vent2.2	5’-tga gac ttg ggc act gtc tg-3’	5’- cct ctg ttg aat ggc ttg ct-3’
cdx4.L	5’-aag ggc agc cta tgg agt tt-3’	5’-gtc cca gat gga tga gga ga-3’
krt12.4.L	5’- cac cag aac aca gag tac -3’	5’- caa cct tcc cat caa cca -3’
vegt.L	5’-caa gta aat gtg aga aac cg-3’	5’-caa ata cac aca cat ttc cc-3’
cdx4.L	5’-aag ggc agc cta tgg agt tt-3’	5’-gtc cca gat gga tga gga ga-3’
ef1a	5’-cag att ggt gct gga tat gc-3’	5’-act gcc ttg atg act cct ag-3’

Primers used for RT-qPCR

Gene name	Forward primer	Reverse primer
tbxt S	5’-tca cta gcc att cat tcc ct -3’	5’-gac tat cga ttc cct cat cc -3’,
wnt8a.L	5’-atg agg tcg ggt aac agt gc -3’	5’-taa tcg gga gag tct tcg ag -3’
wnt8a-like	5’-ttc tgc acc aga aag gaa cg -3’	5’-ac cat ttt aga cat tat ctt -3’
cdx4.L	5’- tga ttt atc acc taa cca g -3’	5’- gtc cca gat gga tga gga ga -3’
nodal3.1.L	5’- ggc aaa agg tct cca tct -3’	5’- cag ctt ctg gcc aag act -3’
admp2.L	5’- ggc ttc ctt gtg atg ttc ac -3’	5’-gc agg taa gac ctt ttg ttg-3’
fgf8b.L	5’-gaa gct gat tgg gaa gac t -3’	5’- gcc ata aac cag cct tcg ta-3’
ef1a.1.S	5’-acc ctc ctc ttg gtc gtt tt -3’	5’-ttt ggt ttt cgc tgc ttt ct -3’
hoxd1.S	5’-ccc tgc aat gtg agg aca aa-3’	5’-gat gcg cct tgc tct tgt g-3’
msgn1.L	5’-gta tcc aac act ttg cca tg -3’	5’-agc act gga gaa ggt ttg tg -3’
pnhd.L	5’- tag ggc tct ggc aca aat g -3’	5’-gct cac aat gtc aca agg aatg-3’